

4th European Summer School on Hydrogen Safety

7-16 September 2009, Corsica, France

<http://hysafer.ulster.ac.uk/esshs/>

FUNDAMENTALS OF HYDROGEN SAFETY ENGINEERING

Prof Vladimir Molkov

Hydrogen Safety Engineering and Research (HySAFER) Centre,

University of Ulster

v.molkov@ulster.ac.uk

- Hydrogen safety engineering: framework and subsystems
- Non-reacting jets
- Jet fires (plus cross-analysis with non-reacting jets)
- Venting of deflagrations
- Hydrogen safety engineering and CFD:
 - Permeation
 - Blowdown of high pressure hydrogen storage
 - Spontaneous ignition of high pressure releases
 - LES of premixed combustion (Ulster's multi-phenomena turbulent burning velocity model)

Contribution of the following HySAFER staff to this presentation is gratefully acknowledged:

- Dr Dmitriy Makarov (permeation, deflagrations, etc.)
- Dr Sile Brennan (fires)
- Dr Maxim Bragin (spontaneous ignitions, non-reacting jets)
- Dr Franck Verbecke (deflagrations)
- Mr Jean-Bernard Saffers (hydrogen safety engineering, permeation, non-reacting jets)

Funding by EC and collaboration of partners within HySafe, HyCourse, HYPER, HySAFEST projects is highly appreciated

Hydrogen Safety Engineering: framework and subsystems

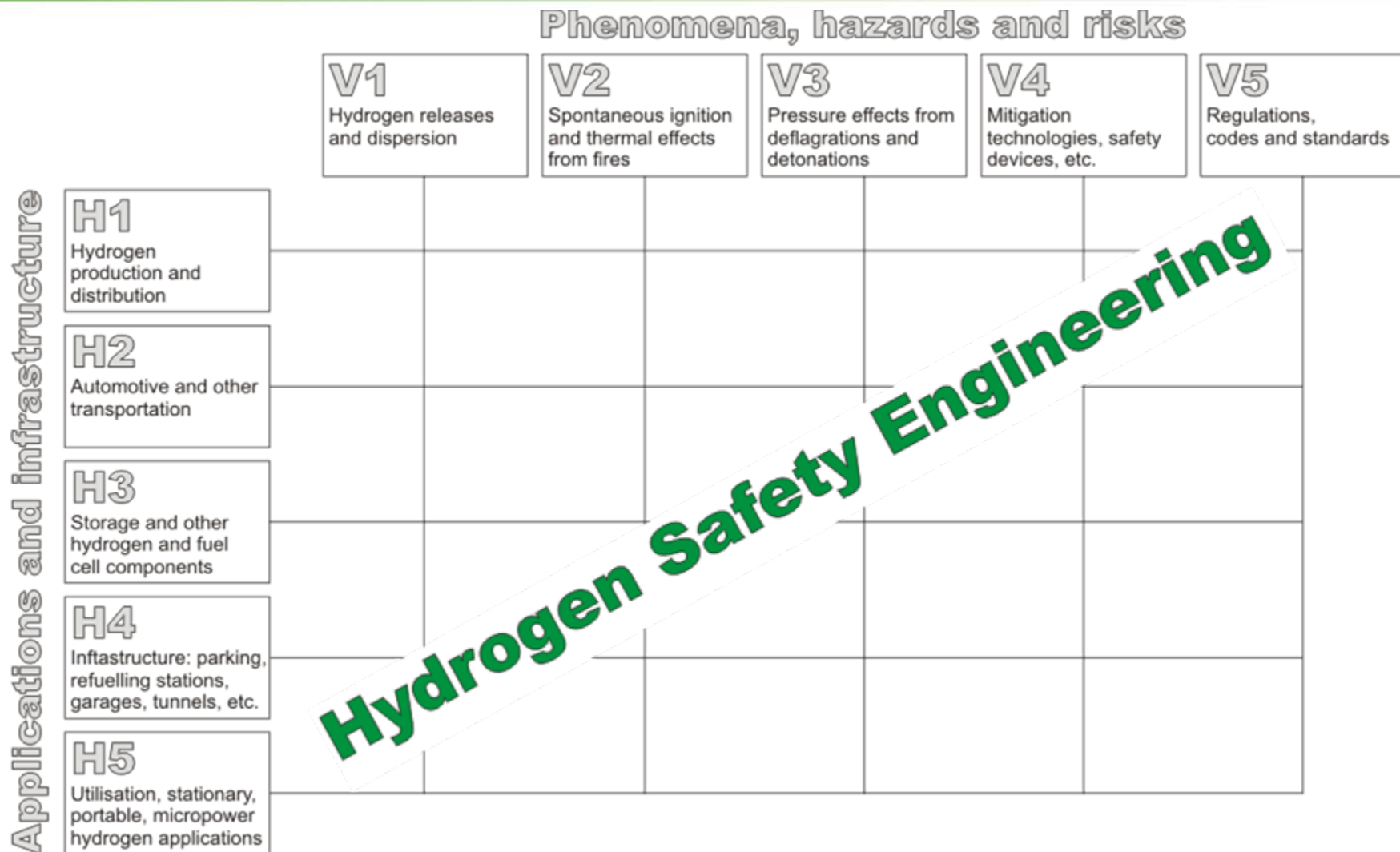


Hydrogen Safety Engineering:
application of scientific and engineering principles to the protection of life, property and environment from adverse effects of incidents/accidents involving hydrogen

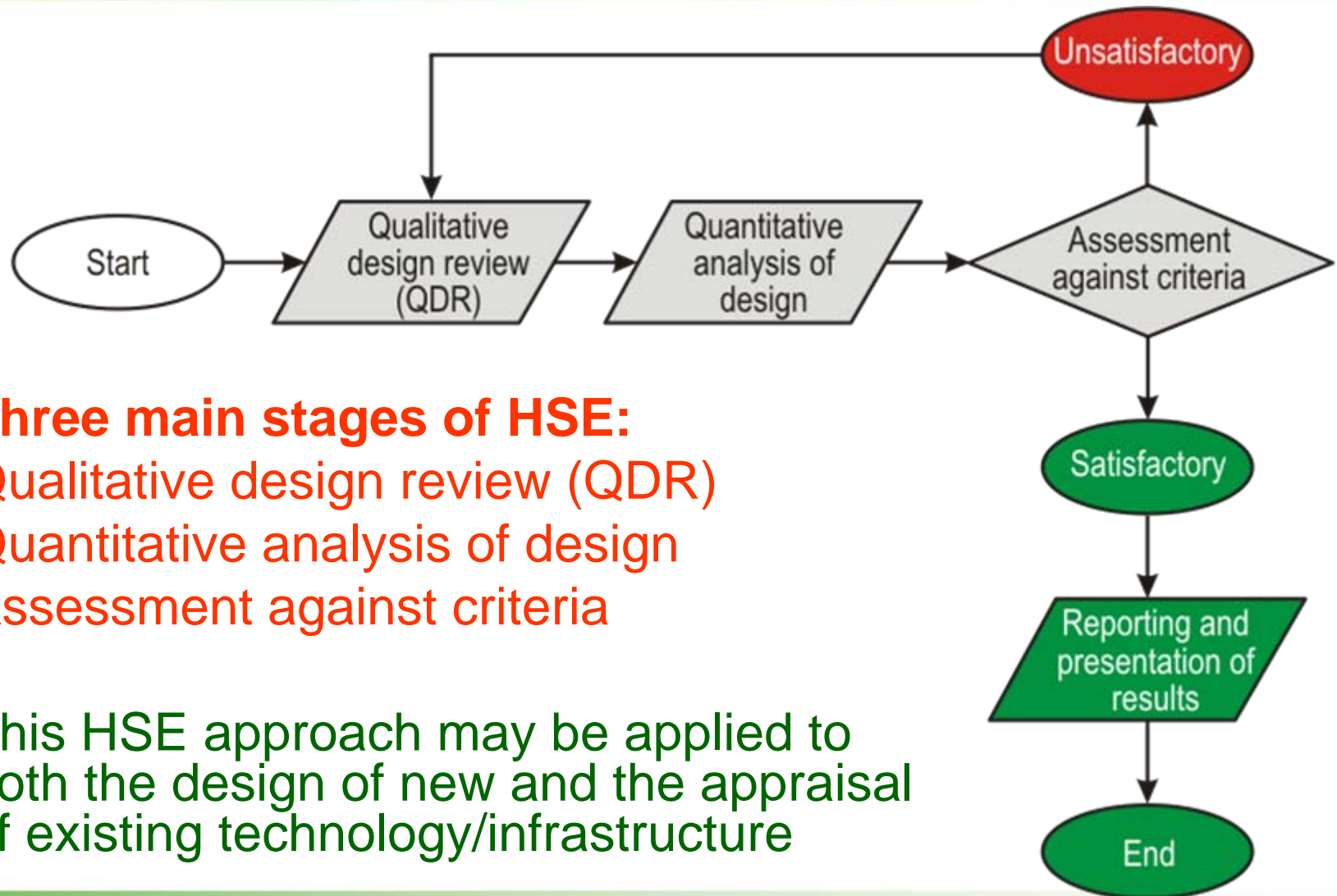
- **Hydrogen hazard**: source of possible injury or damage from hydrogen incident/accident
- **Deterministic study**: methodology, based on physical relationships derived from scientific theories and empirical results that, for a given set of initial conditions, will always produce the same outcome
- **Probabilistic risk assessment**: methodology to determine statistically the probability and outcome of events
- **Approvals body**: organization responsible for approving the hydrogen safety aspects of an infrastructure. Examples of approvals bodies are the local authority building control, approved inspectors, and the emergency services authority.
- **Scenario**: set of circumstances, chosen as an example, that defines the development of incident/accident involving hydrogen

- **Trial safety design**: package of hydrogen safety measures which, in the context of the system/infrastructure, may meet the specified safety objectives
- **Risk**: product of probability of an accident in a given technical operation or state in a defined time, and consequence or extent of damage to be expected on the accident
- **Risk analysis**: systematic use of available information to identify hazards and estimate the risk
- **Risk evaluation**: process of comparing the estimated risk against given risk criteria to determine the significance of the risk
- **Risk assessment**: overall process of risk analysis and risk evaluation

The scope



The process



Three main stages of HSE:

- Qualitative design review (QDR)
- Quantitative analysis of design
- Assessment against criteria

This HSE approach may be applied to both the design of new and the appraisal of existing technology/infrastructure

Three main stages

- **Qualitative design review (QDR):** Review of design; definition of safety objectives; analysis of hazards and consequences; establishment of trial designs; definition of acceptance criteria; scenarios to study are defined. Key information is compiled to evaluate trial safety design in the quantitative analysis (next stage).
- **Quantitative analysis.** Engineering methods and tools are used to evaluate the trial design identified in QDR. Quantitative analysis can be time-based analysis using appropriate sub-system guidelines to give numerical values of the impact of incident/accident, involving hydrogen, on people, property and environment.
- **Assessment against criteria.** The output of the quantitative analysis is compared to the acceptance criteria identified in QDR to ensure the acceptability of the proposal(s). If the safety performance of a hydrogen system/infrastructure does not match acceptance criteria, the design is unsatisfactory and the objectives are not fulfilled, it is necessary to restart a new study from QDR.

To simplify the evaluation of hydrogen safety design, the process should be broken down into sub-systems:

- **SS1: Initiation of release and dispersion**
- **SS2: Ignitions**
- **SS3: Deflagrations and detonations**
- **SS4: Fires**
- **SS5: Impact on people, structure and surroundings**
- **SS6: Detection and mitigation techniques**
- **SS7: Emergency service intervention**

Plus “Guide to hydrogen safety design framework and engineering procedures”

Plus “Guidance on probabilistic hydrogen risk assessment”

QDR: steps

- The Qualitative Design Review (QDR), a ***qualitative process*** that draws upon the *experience and knowledge* of ***the team members***.
- Ideally, the QDR should be carried out ***early in the design*** process so that any substantial findings can be incorporated into the design before the working drawings are developed.
- The following ***steps*** should be taken when conducting the QDR:
 - a) review the technological and architectural design;*
 - b) establish the safety objectives;*
 - c) identify hydrogen hazards and possible consequences;*
 - d) establish trial hydrogen safety designs;*
 - e) identify acceptance criteria and methods of analysis;*
 - f) establish hydrogen accident scenarios for analysis.*

The main **hydrogen safety objectives** that may be addressed are (list is not exhaustive; not all items may be appropriate to a particular study):

- a) life safety;
- b) loss control; and
- c) environmental protection.

The main **life safety objectives** may include provisions to ensure that:

- The occupants are able ultimately to leave the scene of accident in reasonable safety *or the risk* to occupants is acceptably low;
- Emergency services are able to operate in reasonable safety;
- Structure collapse does not endanger people (including firefighters) who are likely to be near the scene.

- **Criteria** should be identified which can be used to assess that *the requirements of legislation have been satisfied*.
- The following **methods** (one or more) can be used to determine criteria against which established designs will be assess:
 - a) **deterministic** (including, when appropriate, safety factors);
 - b) **probabilistic** (risk-based);
 - c) **comparative**;
 - d) **financial** (cost-effectiveness).

For deterministic study The objective is to show that on the basis of the initial assumptions (scenarios), a ***defined set of conditions will not occur***. Generally, ***life safety criteria*** should be set to ensure that a safety solution offers at least the same level of safety as similar exiting technologies.

- **For probabilistic studies.** The objective is usually to show that *the likelihood of a given event occurring* (e.g. injury, death, large life loss, large property loss and environmental damage) is acceptably or tolerably small. **A full probabilistic study** is only likely to be justified when a **substantially new approach** to infrastructure design or hydrogen safety practice is being adopted.
- **For comparative studies** The objective is to demonstrate that the infrastructure, as designed, presents **no greater safety issues** to the occupants than a similar infrastructure complying with a **well established code**. In many projects it is likely that the provisions of existing codes of practice and other guidance will be largely followed and that hydrogen safety engineering techniques will not be necessary, or may be used **only to justify limited departures** from the codes. **A safety design analysis using comparative criteria will generally require fewer data** and resources than a probabilistic approach and is likely to be the simplest method of achieving an acceptable design.

QDR: fire scenarios

- The detailed analysis and quantification of accident scenarios for a specific technology/infrastructure should be **limited to the most significant** hydrogen accident scenarios. In a deterministic or comparative study it is usual to identify a number of **worst-case** scenarios for further evaluation.
- **The QDR team** should establish the important **scenarios to analyse** and those that **do not require analysis**. Events with a very low probability of occurrence should not be analysed **unless their outcome is potentially catastrophic** and a **reasonably practicable remedy is available**.
- **The qualitative analysis** should identify the important fire development scenarios and describe them **in a manner suitable for the quantification process**.

- This is the **second of three main steps** of the hydrogen safety engineering process.
- **The examples** of simple engineering methods and CFD simulations to be used during this step are described further in this lecture:
 - The similarity law for non-reacting momentum jets
 - The correlation and nomogram for jet fire length
 - The correlations for vented deflagrations
 - Permeation
 - Blowdown of high pressure hydrogen storage
 - Spontaneous ignition of high pressure releases
 - LES of premixed deflagrations

- Following the quantitative analysis based on the sub-systems, ***the results should be compared with the acceptance criteria identified during the QDR.*** Three basic types of approach can be considered:
 - a) deterministic;
 - b) probabilistic;
 - c) comparative.
- If, following the quantitative analysis, it is demonstrated that ***none of the trial safety designs satisfies*** the specified acceptance criteria, the ***QDR and quantification process should be repeated*** until a hydrogen safety strategy has been found that satisfies acceptance safety criteria and other design requirements (see Figure before on the process of hydrogen safety engineering).

- ***In a deterministic study*** the objective is to show that on the basis of the initial (usually “worst credible” case) assumptions a defined set of conditions will not occur. It should be assessed (***life safety***) that all persons ***can sustain and/or leave*** a threatened part of an infrastructure in reasonable safety without assistance. Where the ***failure of the system/infrastructure***, in particular structural failure, will threaten the life, adequate ***fire and explosion resistance*** should be provided.
- ***In a probabilistic study***, such criteria are set that the probability of a given event occurring is acceptably low. The risk criteria are usually expressed in terms of the annual probability of the unwanted event occurring.

Hydrogen safety engineering benefits:

- Provides the hydrogen safety engineer with a disciplined approach to hydrogen safety design;
- Allows the safety levels for alternative designs to be compared;
- Provides a basis for selection of appropriate hydrogen safety strategies;
- Provides opportunities for innovative design;
- Provides information on the management of hydrogen safety for a system and/or infrastructure.

Non-reacting hydrogen jets



- The following formula, within the experimental accuracy of about +20% is a precursor to the similarity law of Chen and Rodi (CR, 1980)

$$C_{ax} = 5 \cdot D_{eff} / x \qquad D_{eff} = D \sqrt{(T_S / T_N)(\rho_N / \rho_S) P_c}$$

Thus, there are two difference with the similarity law of CR (1980): constant is 5.4 instead of 5.0, and square root from temperature ratio is not present in CR (1980)

$$C_{ax} = 5.0 \sqrt{\frac{\rho_N}{\rho_S}} \frac{D}{x} \sqrt{\frac{T_S}{T_N}}$$

- “Calculated flame length may be obtained by substitution the concentration corresponding to the stoichiometric mixture in equation of axial concentration decay for non-reacting jet”...

- Study of entrainment into jets with high Reynolds numbers and at distances with large length to diameter L/D ratio.
- Dimensional analysis: **the mass flow rate**, including entrained air, at right angle to the jet axis is **proportional to distance x** (M_0 - momentum flux of the jet at orifice)

$$m(x) = K_1 M_0^{1/2} \rho_S^{1/2} x$$

- Experimentally proved that this equation holds for non-uniform density **provided that buoyancy effects are negligible**. Experimental data obey the relation (isothermal injection of hydrogen, propane, carbon dioxide)

$$\frac{m(x)}{m_N} = 0.32 \frac{x}{D} \sqrt{\frac{\rho_S}{\rho_N}}$$

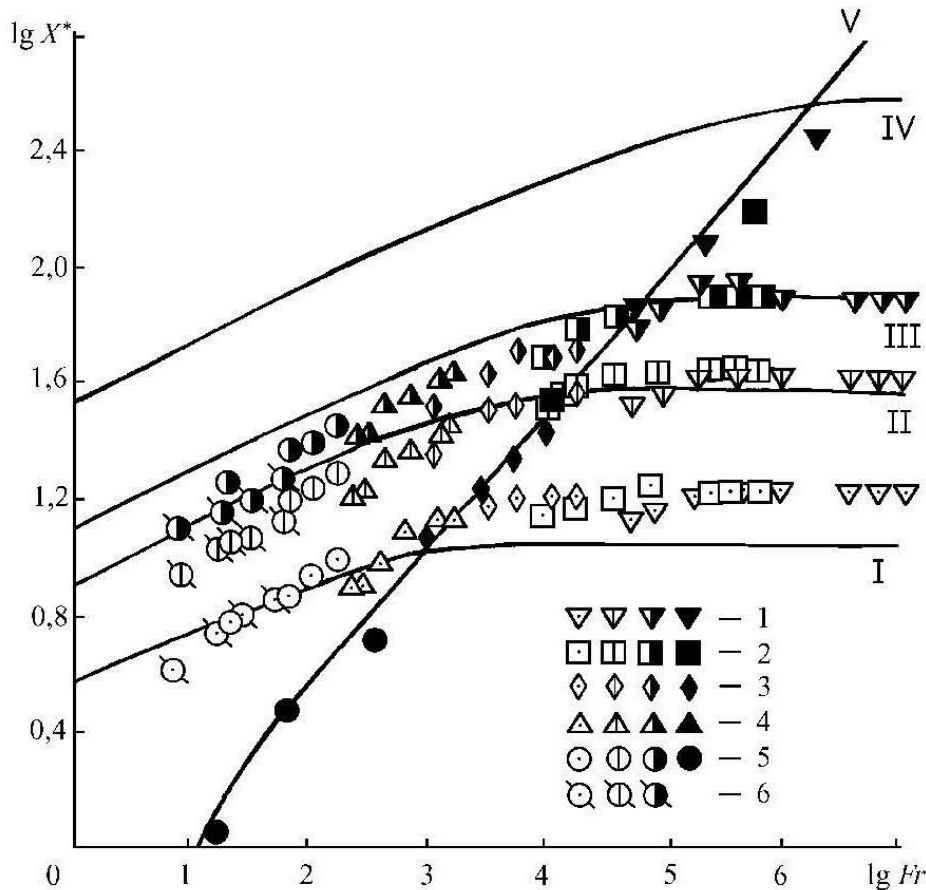
- Reciprocal to the left-hand side of the previous equation by Ricou and Spalding (1961) is a **fuel mass fraction averaged through the jet cross-section**

$$C_{av} = 3.1 \sqrt{\frac{\rho_N}{\rho_S}} \frac{D}{x}$$

- Axial** mass fraction (the similarity law by Chen and Rodi for round jets)

$$C_{ax} = 5.4 \sqrt{\frac{\rho_N}{\rho_S}} \frac{D}{x}$$

- Conclusion from papers** by Sunavala et al. (1957), Ricou and Spalding (1961), and Chen and Rodi (1980): *Flammable envelope increases proportional to nozzle diameter.*
- Something to remember (expanded H2 jets): $(L/D)_{8.5\%} = 222$



Axes: $X^*=L/D$; $Fr=U^2/gD$

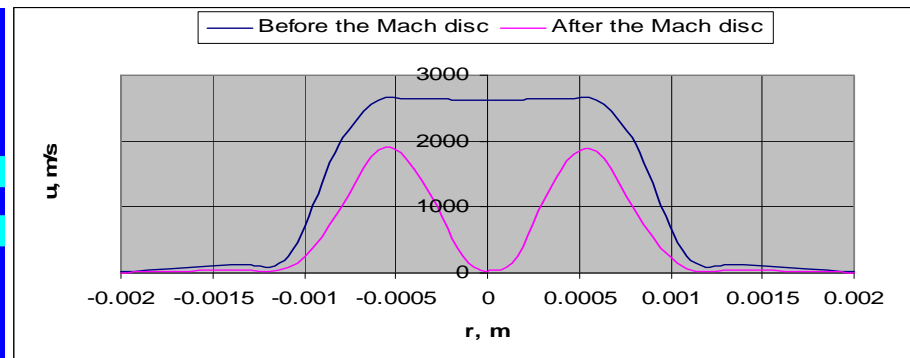
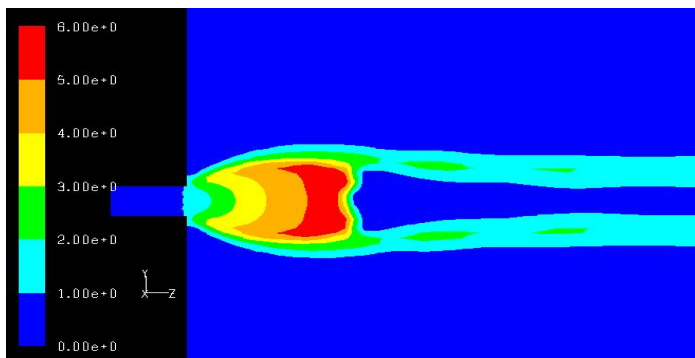
Рис. 2. Зависимость безразмерного расстояния по оси струи водорода до точки с концентрацией c от числа Фруда: кривые — расчет, точки — эксперимент; I — для $c = 60\%$ по объему; II — 30% , значки с чертой; III — 17% , полузачерненные; IV — 4% ; V — длина струи вертикально вниз до точки возврата; d_0 , мм: 1 — 6; 2 — 10,2; 3 — 20,8; 4 — 32; 5 — 52; 6 — 96

**I — 60% by volume (symbols with a dot); II — 30% (line); III — 17% (half black); IV — 4%; V — downwards jet length until reverse point (black).
 D , mm: 1 — 6; 2 — 10.2; 3 — 20.8; 4 — 32; 5 — 52; 6 — 96.**

- Shevyakov et al. (1980) showed that at high Froude numbers $Fr > 10^5$ ($Fr = U^2/gD$) the relative distance to 30% by volume of hydrogen $(L/D)_{30\%}$ is a constant equal to 47.9. This is an excellent agreement with Chen and Rodi (1980) value 49.3. The difference between two independent methods is within 3%.
- Similar agreement for the size of flammable envelope size:
 $(L/D)_{4\%} = 410$ (theory Shevyakov et al., 1980),
 $(L/D)_{4\%} = 494$ (Chen and Rodi correlation, 1980)
- Hydrogen concentration is not changing from nozzle until distance $x = 4.5D$.
- **Are conclusions made for expanded jets valid for underexpanded jets at storage pressure up to 700 bar (onboard car storage) and 1000 bar (refuelling)?**

Underexpanded jets

- Jet is considered underexpanded if the pressure at the end of a nozzle has not fully dropped to the atmospheric pressure. The exit velocity remains locally sonic.
- Ishii et al., 1999:
 - Subsonic matched jets* for ratios of pressure in high-pressure and low-pressure chambers (the only parameter controlling the jet strength) between 1 and 4.1;
 - Sonic underexpanded jets* for pressure ratios in the range from 4.1 to 41.2; and
 - Supersonic underexpanded jets* for pressure ratios > 41.2 .



- Natural gas (2-70 bar). Notional nozzle diameter

$$D_{eff} \propto D \sqrt{p_R / p_S}$$

- Mean volume fraction (subcritical natural gas: $x_0 = -3.6$; supercritical: $x_0 = -0.1$)

$$C_{ax} = 4.9 \sqrt{\frac{\rho_S}{\rho_N}} \frac{D_{eff}}{x + x_0}$$

- Birch et al., 1987, for relatively high pressures ($x_0 = 0.6D$ being small):

$$C_{ax} = 5.4 \sqrt{\frac{\rho_S}{\rho_N}} \frac{D_{eff}}{x} \quad \text{with} \quad \frac{D_{eff}}{D} = \sqrt{\frac{p_R}{p_S} \left(\frac{2}{\gamma+1} \right)^{1/(\gamma-1)} \frac{1}{(\gamma+1)}}$$

- “Similar looking” formulas by Chen and Rodi (1980) and Birch et al. (1987)?

$$C_{ax} = 5.4 \sqrt{\frac{\rho_N}{\rho_S}} \frac{D}{x} \quad (1980) \qquad C_{ax} = 5.4 \sqrt{\frac{\rho_S}{\rho_N}} \frac{D_{eff}}{x} \quad (1984)$$

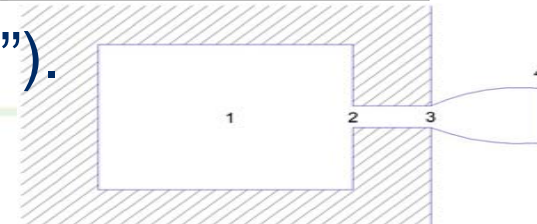
- No! There are THREE PRINCIPLE DIFFERENCES:
 1. Volume fraction (1987) instead of mass fraction (1980)
 2. Density ratio is reciprocal to the original similarity law
 3. Notional nozzle (1987) instead of real nozzle (1980)
- **The ambiguity in use of the similarity law for underexpanded jets by hydrogen safety community**
- Let us validate the similarity law for high pressure releases (underexpanded jets)

Underexpanded jet theory

- Unfortunately, Birch et al. (1984) and similar approaches (Evan and Moodie, 1986) can not be applied for $p > 100$ bar

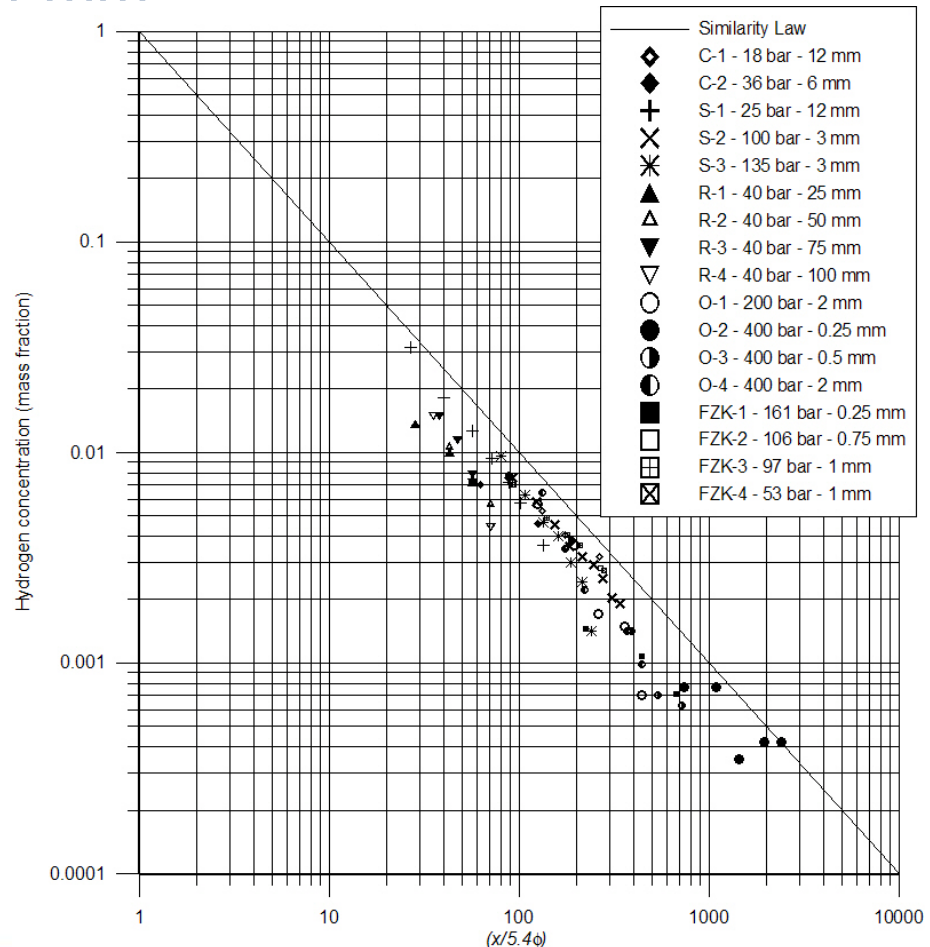
$\rho_1 = \frac{p_1}{bp_1 + R_{H2}T_1}$	$u_4 = a_4 = \sqrt{\gamma R_{H2}T_4} \quad \text{Assumption}$
$c_p T_1 = c_p T_3 + \frac{u_3^2}{2}$	$\rho_4 = \frac{p_4}{R_{H2}T_4}$
$\rho_3 = \frac{p_3}{bp_3 + R_{H2}T_3}$	$c_p T_3 + \frac{u_3^2}{2} = c_p T_4 + \frac{u_4^2}{2}$
$u_3^2 = a_3^2 = \frac{\gamma p_3}{\rho_3(1 - b\rho_3)}$	$\rho_3 u_3 A_3 = \rho_4 u_4 A_4$
$p_1 \left(\frac{1}{\rho_1} - b \right)^\gamma = p_3 \left(\frac{1}{\rho_3} - b \right)^\gamma$	Unknown parameters: $\rho_1, \rho_3, u_3, T_3, p_3, \rho_4, u_4, T_4, A_4$. Know parameters: p_1, T_1, A_3, p_4 and constants c_p, R_{H2}, b, γ .

- The Abel-Noble equation (700 bar “– 50%”).



Experimental data

- **Chaineaux et al. (1991):** $V=0.12 \text{ m}^3$ ($D=55 \text{ cm}$, $L=55 \text{ cm}$), $p=100 \text{ bar}$, orifice $D=5, 12, 24 \text{ mm}$
- **Ruffin et al. (1996):** $V=5 \text{ m}^3$, $p=40 \text{ bar}$, $D=25-100 \text{ mm}$
- **Shirvill et al. (2005-2006):** $p=10-172 \text{ bar}$, $D=1-12 \text{ mm}$
- **Okabayashi et al. (2005):** $p=400 \text{ bar}$, $D=0.25-2 \text{ mm}$
- **Kuznetsov et al. (2006):** $p=53-161 \text{ bar}$, $D=0.16-1 \text{ mm}$



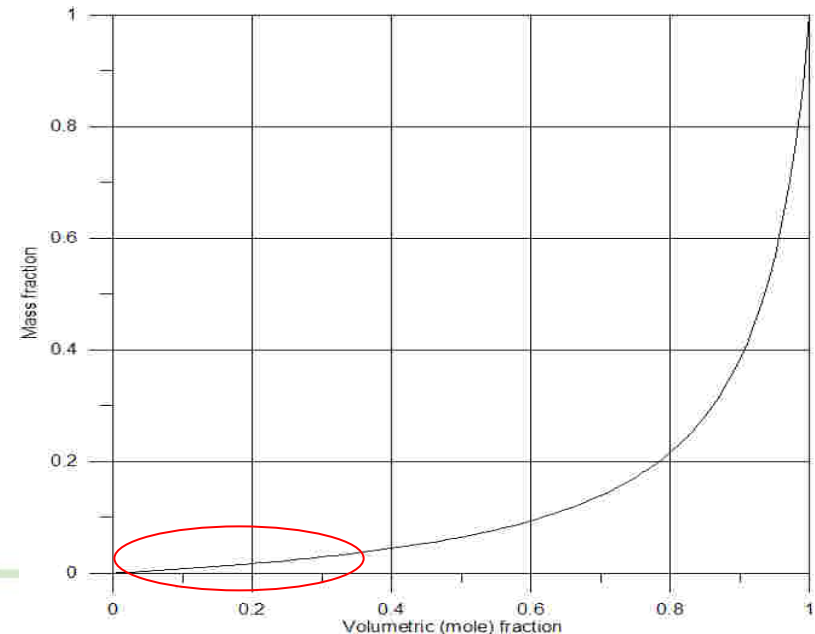
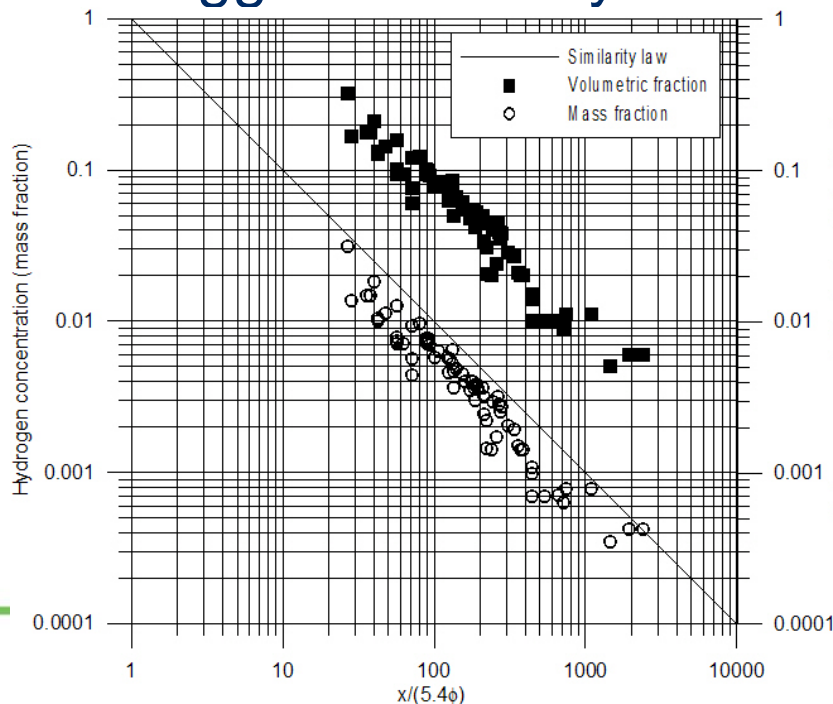
Mass fraction!

There are at least ***five possible reasons*** for higher calculated concentrations (dotted line – the similarity law) compared to experimentally measured concentrations :

- *The first* is absence of losses in the applied theory.
- *The second* is a possible decrease of initial storage pressure immediately after the start of release as observed in some experiments of such kind (Schefer et al., 2007).
- *The third* reason is buoyancy due to horizontal direction of jet whereas the original correlation is for vertical jets.
- *The fourth* is use of “spouting” pressure rather than pressure in the reservoir with stagnant hydrogen, i.e. static pressure is used for calculations rather than total pressure (dynamic pressure in many situation can not be neglected).
- *The fifth* – coefficient in the correlation (CR) is conservative

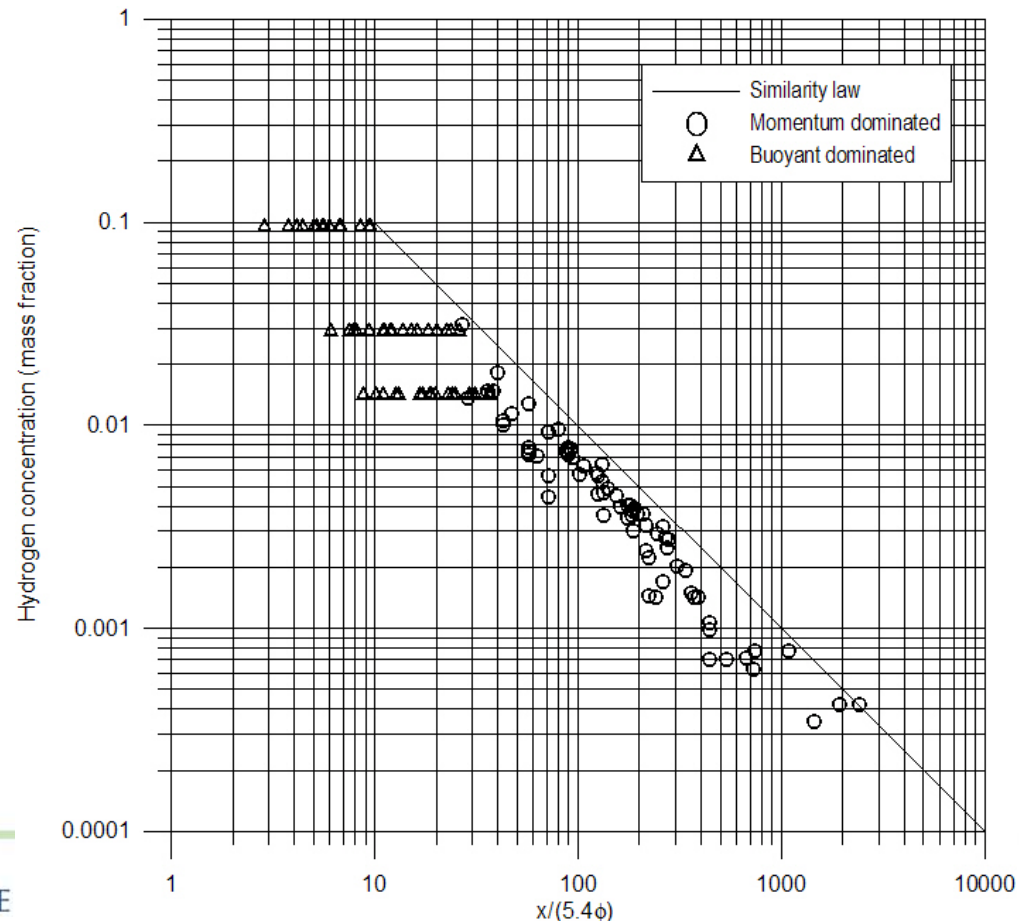
Mass vs volume fraction

Concluding remark: the original correlation by Chen and Rodi (1980) works for both expanded and underexpanded jets (**momentum controlled regime** according to derivation assumptions, e.g. Ricou and Spalding, 1961) *if the density of underexpanded jet in the nozzle is calculated accounting for non-ideal behaviour of hydrogen at high pressures, e.g. by the suggested theory. Volume fraction should not be used!*



The original correlation by Chen and Rodi (1980) *works* for **momentum controlled regime** accurately and overpredicts for buoyant jets (too large safety distances).

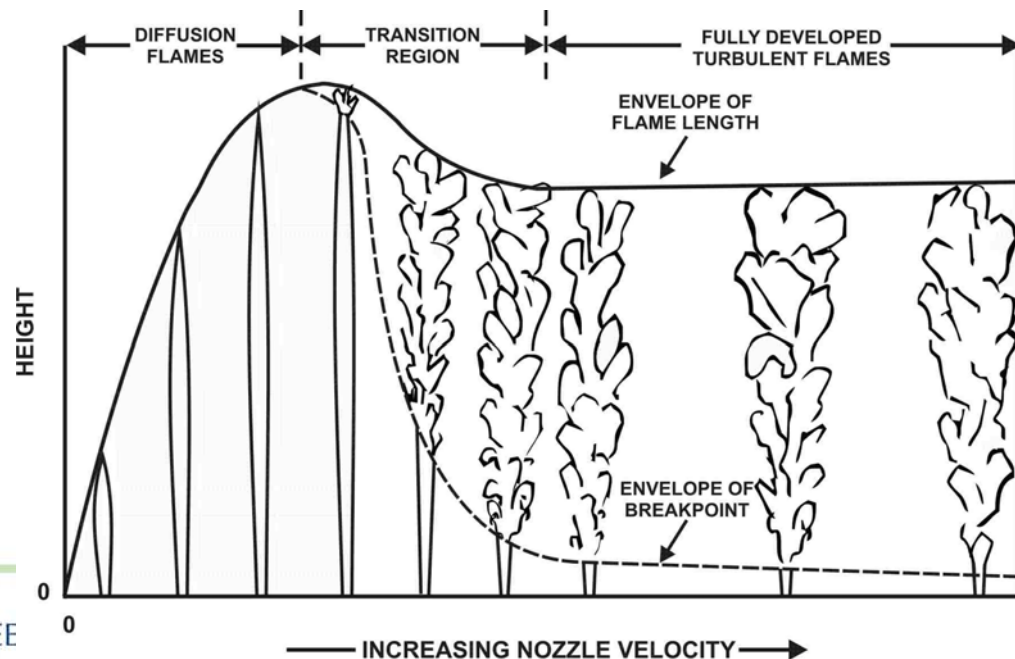
**Hydrogen Safety
Engineering reduces
safety distances!**



Hydrogen jet fires



- The classic theoretical consideration of mixing and combustion in turbulent gas jets by Hawthorne, Weddell, Hottel (HWH).
- “The process of *mixing* is the controlling factor in determining progress of the combustion”.
- Transition from laminar diffusion to turbulent flames commences for release of hydrogen into still air at Reynolds number around 2000 (Hottel, Hawthorne, 1949).



- HWH demonstrated by simple scaling technique that flame length L is **proportional to diameter D** only and concluded that ***fuel gas flow rate is no factor***, as long as it is great enough to produce a fully developed turbulent flame

$$\frac{L_F - s}{D} = \frac{5.3}{C_{st}} \sqrt{\frac{T_{ad}}{\alpha_T T_N} \left[C_{st} + (1 - C_{st}) \frac{M_S}{M_N} \right]}$$

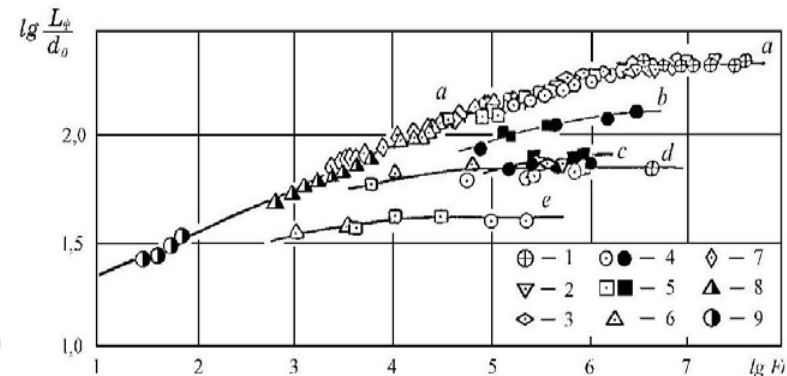
- The visible length observed in the darkened room was 10% greater than that observed in the lighted room.
- For *free turbulent hydrogen flames* in air in which the effects of buoyancy are small, i.e. high orifice velocity and small diameter (in the momentum limit with negligible value of parameter s), and with $\alpha_T=1.173$, $T_{ad}/T_N=8.04$, $C_{st}=0.296$, $M_S/M_N=14.45$, formula casts as
 $L_F/D=152$

- 1949, HWH: $L_F/D=152$
- 1972, Golovichev, Yasakov: **220** (theory), max **205** (365 m/s)
- 1974, Baev et al.: **230** (subsonic laminar), **190** (turbulent limit)
 $L_f/L_t=1.74$ (theory), i.e. expected scattering $\pm 30\%$.
- 1977, Shevyakov et al.: momentum controlled limit **220-230**
- 1993, Delichatsios: **210**
- 1999, Heskestad: **175** (230 – CH₄, 350 – C₃H₈, 50 – CO)
- 2005, Mogi et al.: $L_F/D=524 \cdot P^{0.436}$ (**200**, 0.11 MPa; **254**, 0.19)
- No contradiction – modified Shevyakov’s correlation:

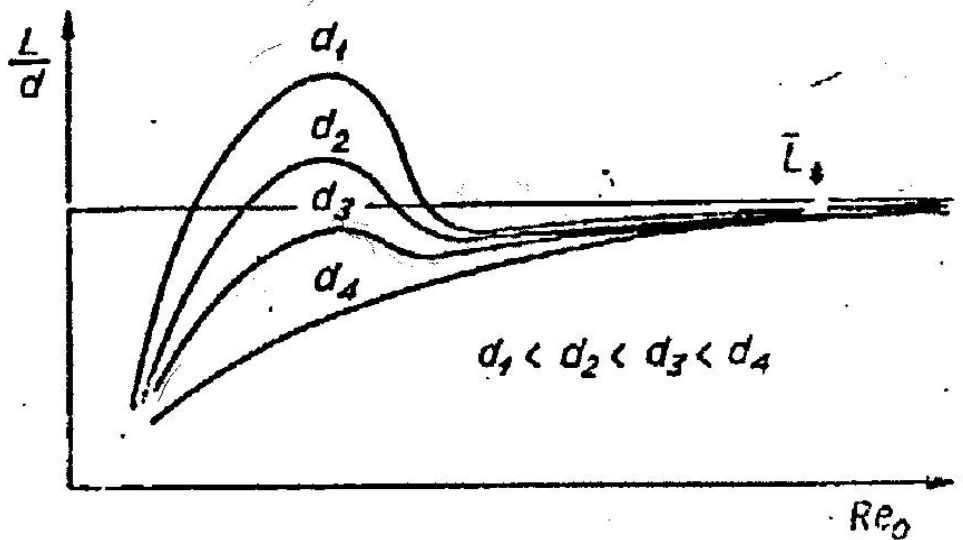
$$L_F / D = 15.8 \cdot Fr^{1/5} \quad (Fr = U^2 / gD < 10^5);$$

$$L_F / D = 37.5 \cdot Fr^{1/8} \quad (10^5 < Fr < 2 \cdot 10^6);$$

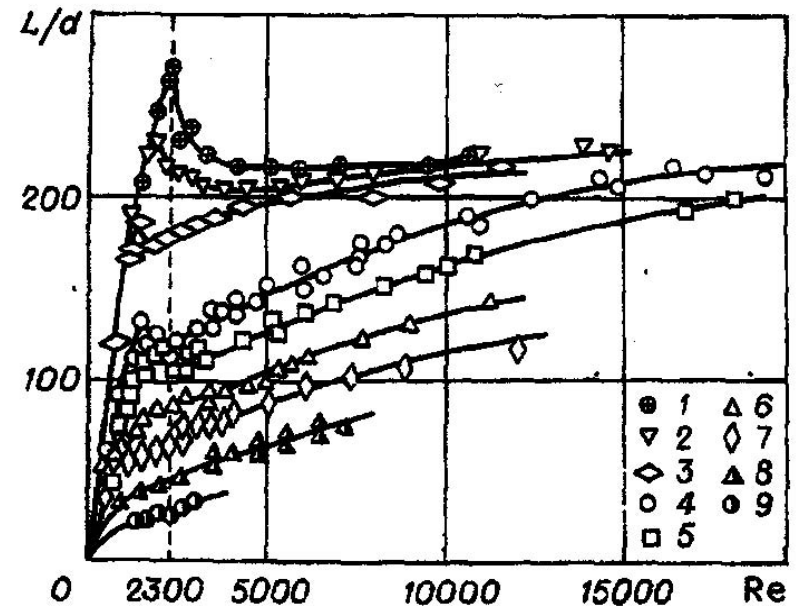
$$L_F / D = 230 \quad (Fr > 2 \cdot 10^6).$$



- Dependence of the flame length to diameter ratio (L_f/D) on Reynolds number for different nozzle diameters, i.e. Fr
- Turbulent flame length limit L_t



Baev, Yasakov (1974, theory)

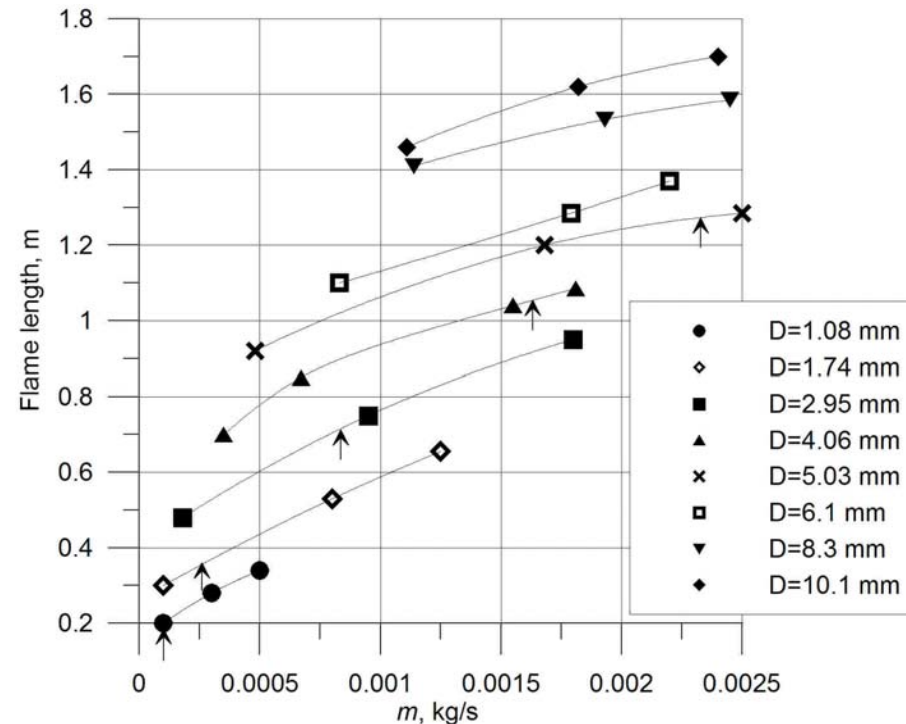


Shevyakov, Komov (1977):
1 – 1.45 mm; 9 – 51.7 mm.

- Can all these scattered data be correlated by one curve?

Flame length grows with mass flow rate for a constant diameter, and with diameter for a constant mass flow rate

Lift-off height varies linearly with the jet exit velocity and is independent of the burner diameter



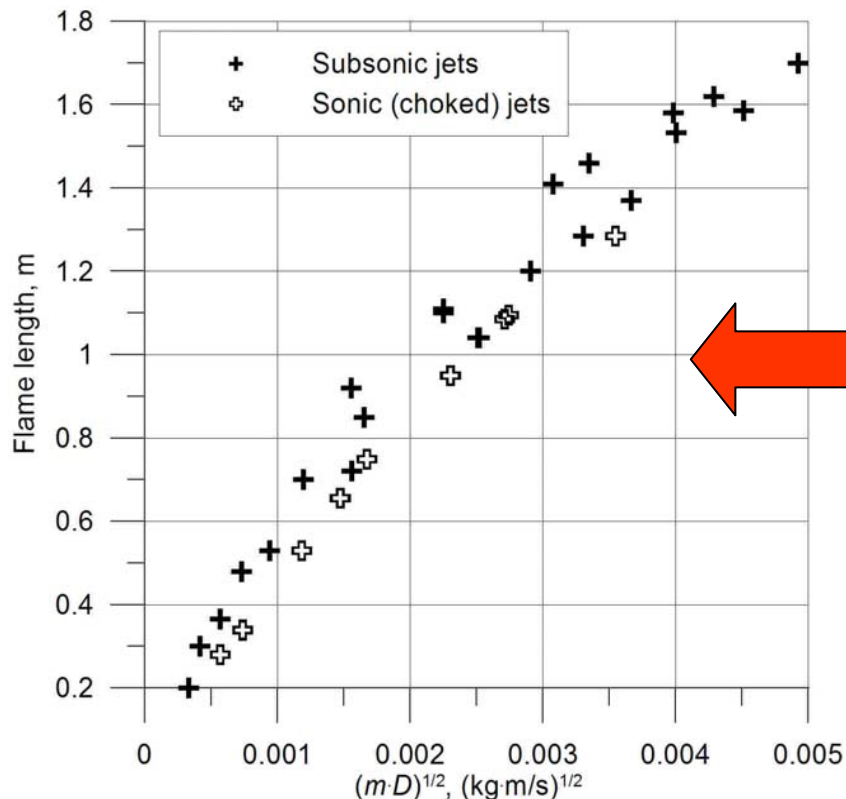
- Cheng and Chiou (1998): *liftoff velocity increases the liftoff height without significant altering the flame height*

- Let us apply dimensional analysis to correlate a flame length, L_F , with a nozzle diameter, D , densities of hydrogen in the nozzle, ρ_N , and density of surrounding air, ρ_S , viscosity, μ , and hydrogen velocity in the nozzle, U .
- The Buckingham theorem (6-3=3):

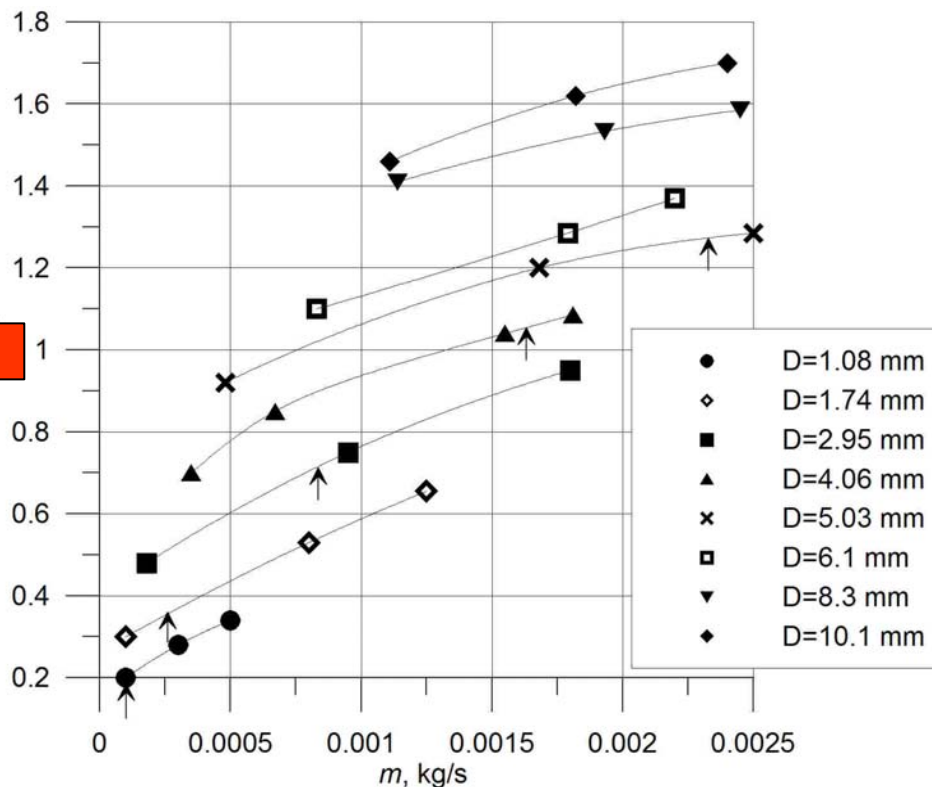
$$L_F = f \left(\dot{m}^{1/2} D^{1/2} \sqrt{\frac{4}{\pi\mu}} \cdot \sqrt[4]{\frac{\rho_S}{\rho_N}} \right)$$

- Let us correlate Kalghatgi data on L_F with new similarity group mD (not just m as in work by Mogi et al., 1995, with $L_F=20.25 \cdot m^{0.53}$ regardless of the nozzle diameter).

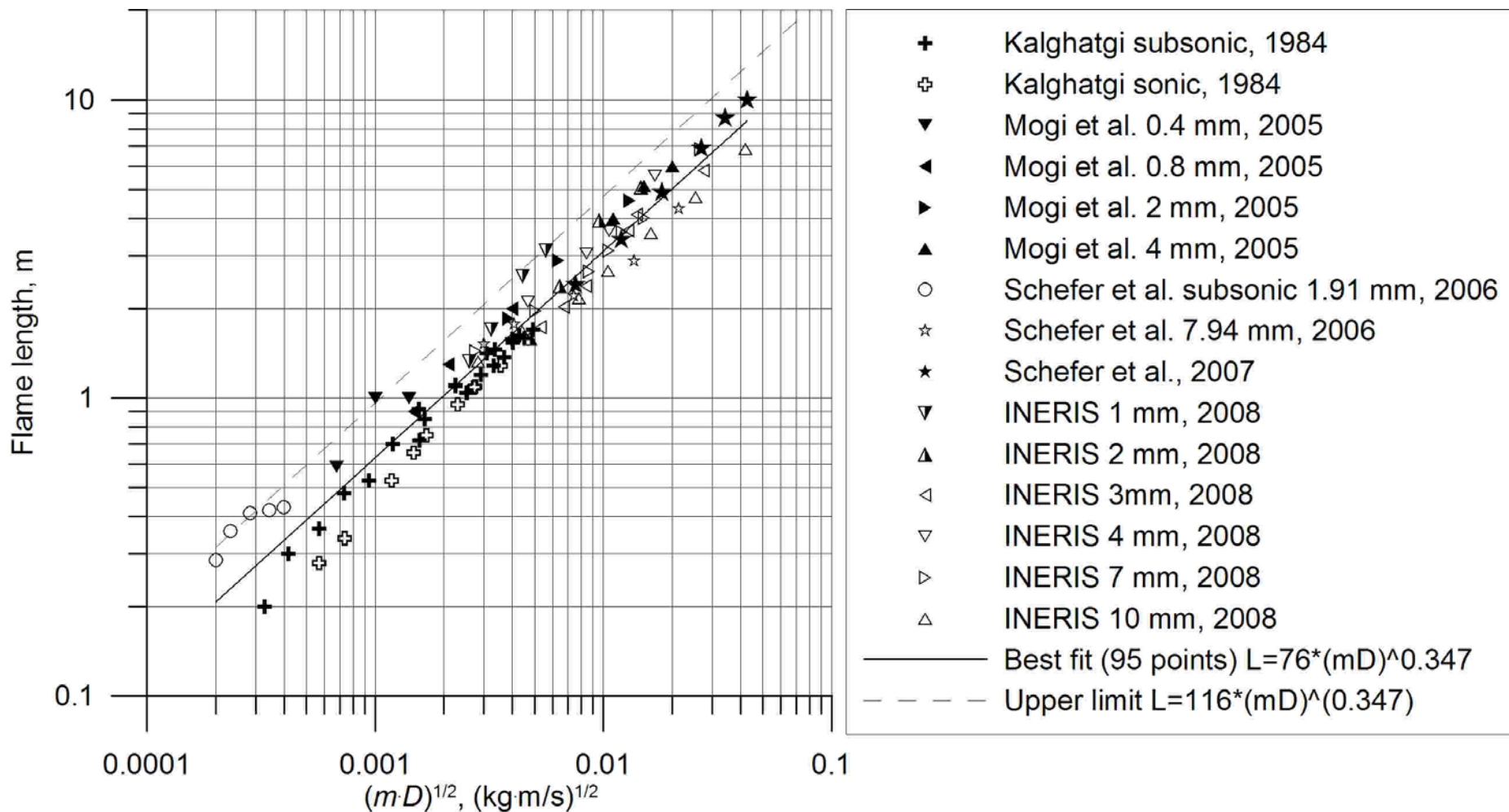
Converged (mD)



Scattered (m)



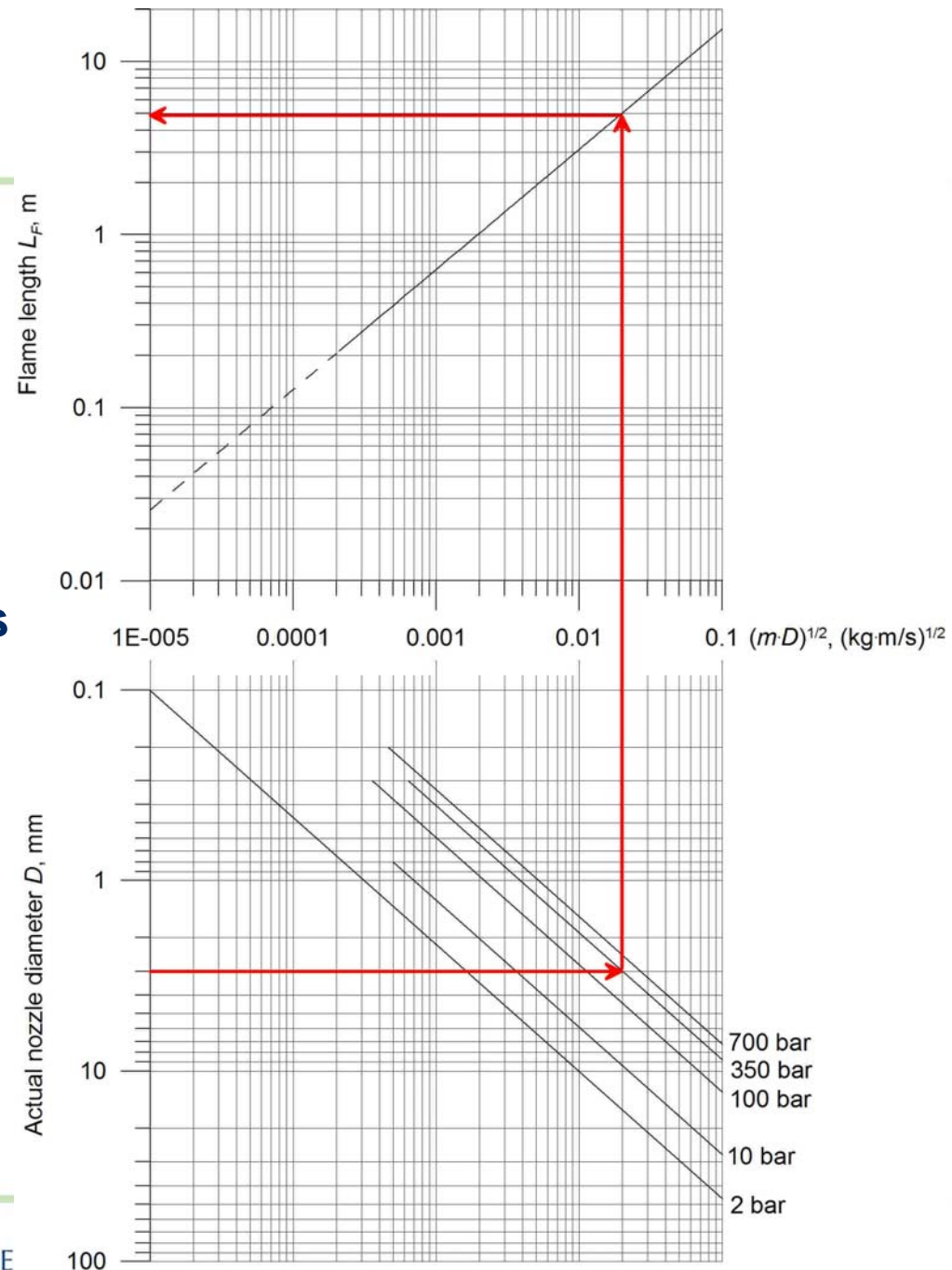
(without dependence on density ratio ρ_S/ρ_N)



The nomogram

for hydrogen safety engineering

Special feature of the nomogram:
Mogi et al., 2005: No stable flames were observed for nozzle diameters 0.1 and 0.2 mm – flame blew off although the spouting pressure increased up to 400 bar.



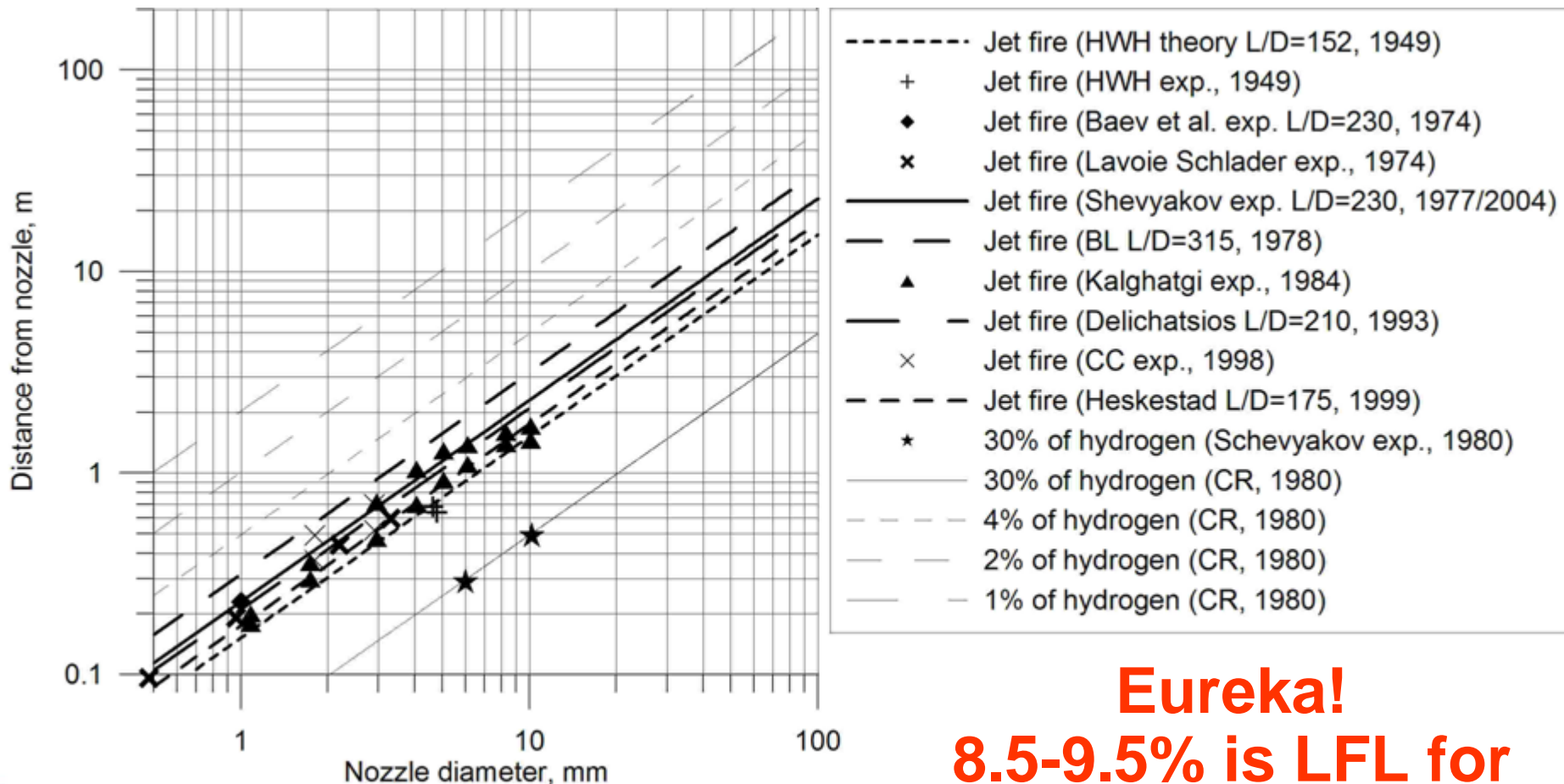
Cross-analysis (non-reacting jets and jet fires)

2-3

- *Hawthorn et al. (1949)* pointed out that it does not follow that burning will proceed as far as ideal mixing would allow. They stated that concentration fluctuations in turbulent flame or local “**unmixedness**”, producing a statistical smearing of reaction zone and a consequent *lengthening beyond the point where the mean composition of mixture is stoichiometric*.
- The performed in this paper comparison of the Chen and Rodi’s similarity law (1980) for non-reacting momentum jets and Schevyakov’s correlation (1977) for hydrogen jet fires at momentum controlled limit revealed that $L_F/D = L_{8.5\%}/D$, i.e. flame tip location corresponds location of mean 8.5% of hydrogen in non-reacting jet from the same nozzle.
- This surprisingly corresponds to the limit of 8.5-9.5% for downward and spherically propagating premixed hydrogen-air flames (see next slide).

Where is the flame tip (2/2)?

Best fit flame length line $L/D=230$ coincides with **8.5%** by volume of hydrogen line $L/D=222$ (non-reacting jet)



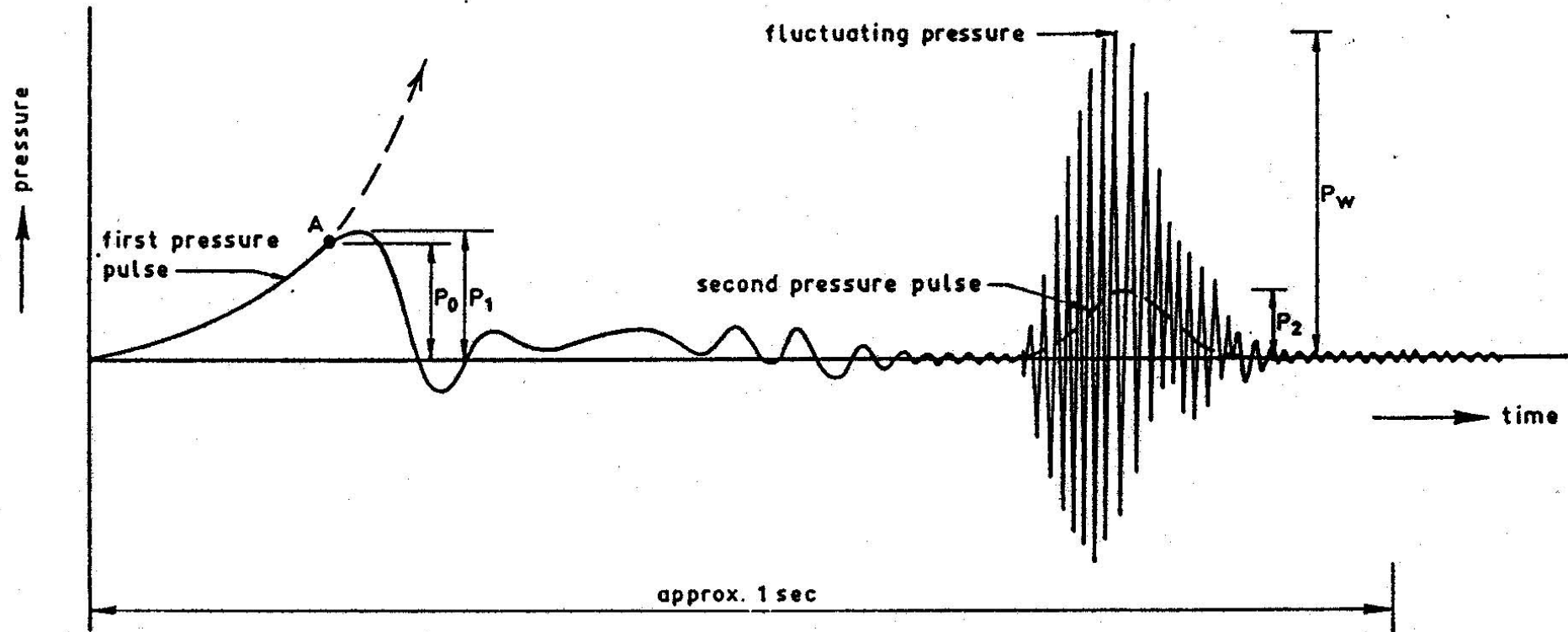
Eureka!
8.5-9.5% is LFL for downward flames!

- The similarity law for non-reacting jets is applicable for both expanded and underexpanded jets **in momentum controlled** regime when the density in the nozzle is calculated by the phenomenological theory of underexpanded jet accounting for non-ideal behaviour of hydrogen by the Abel-Noble equation, e.g. the theory developed at the University of Ulster.
- The novel correlation for hydrogen flame length is developed and validated against 95 experiments at different conditions.
- For the first time it is revealed that for turbulent hydrogen flames in momentum control regime **the flame tip location** for reacting jet is exactly the same as axial **location of 8.5% by volume of hydrogen in non-reacting jet**.
- The nomogram for hydrogen safety engineers is developed.

Venting of deflagrations



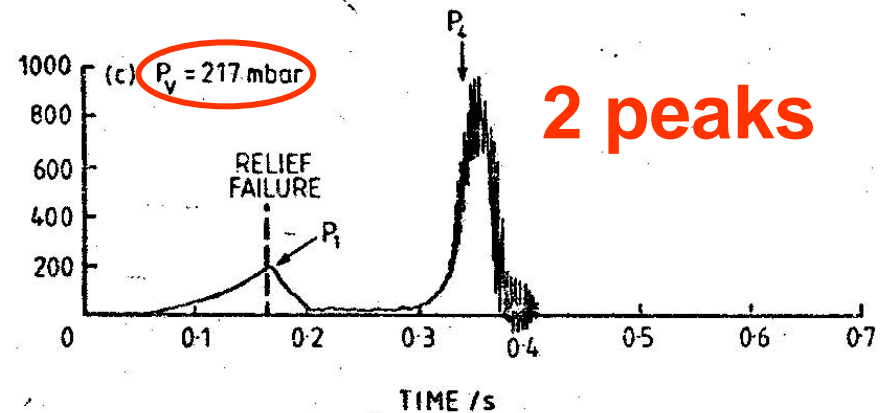
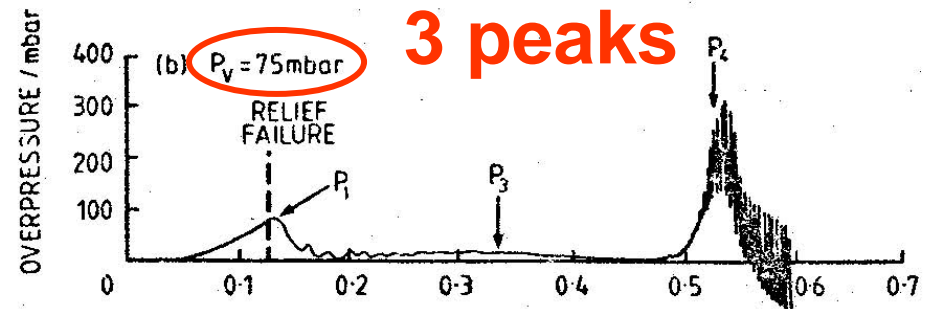
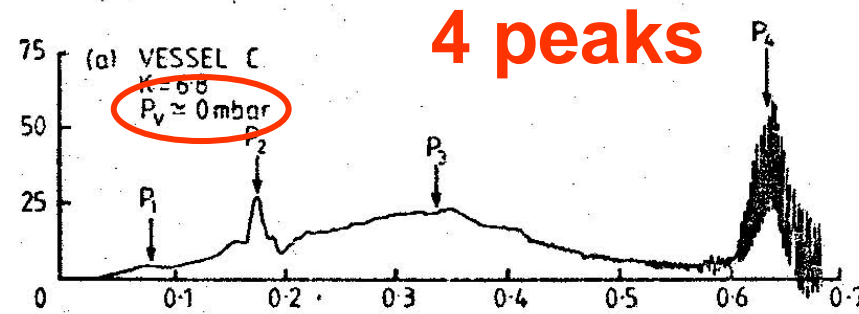
Example: Dragosavic (1973)



Four peaks structure

Cooper et al. (1986):

- P_1 - vent opening, venting of unburned gas then burned;
- P_2 - “external explosion” or highly turbulent combustion of unburned mixture pushed out of the vessel;
- P_3 - decrease of flame front area after flame touches the enclosure walls;
- P_4 - pressure waves resulting from the combustion process couple with the acoustic modes of the vessel and set up sustained pressure oscillations (thus satisfying the Rayleigh criterion)



- It is well known today that vent opening will facilitate the distortion of flame front due to different reasons: front instabilities, including Rayleigh-Taylor, Kelvin-Helmholtz, and acoustic, development of its cellular and then fractal structure, effect of flow turbulence and selective diffusion, and large-scale flame front–flow interactions, etc.
- As a result, the turbulent burning velocity in vented deflagration is known to exceed its value for laminar spherical flame up to 100 times.
- The *turbulence factor* χ is a widely accepted concept that characterises the augmentation of the burning rate (flame front area with respect to the ideal case of laminar spherical flame propagation).
- Until 1995 the data on the turbulence factor obtained by different authors were not correlated.

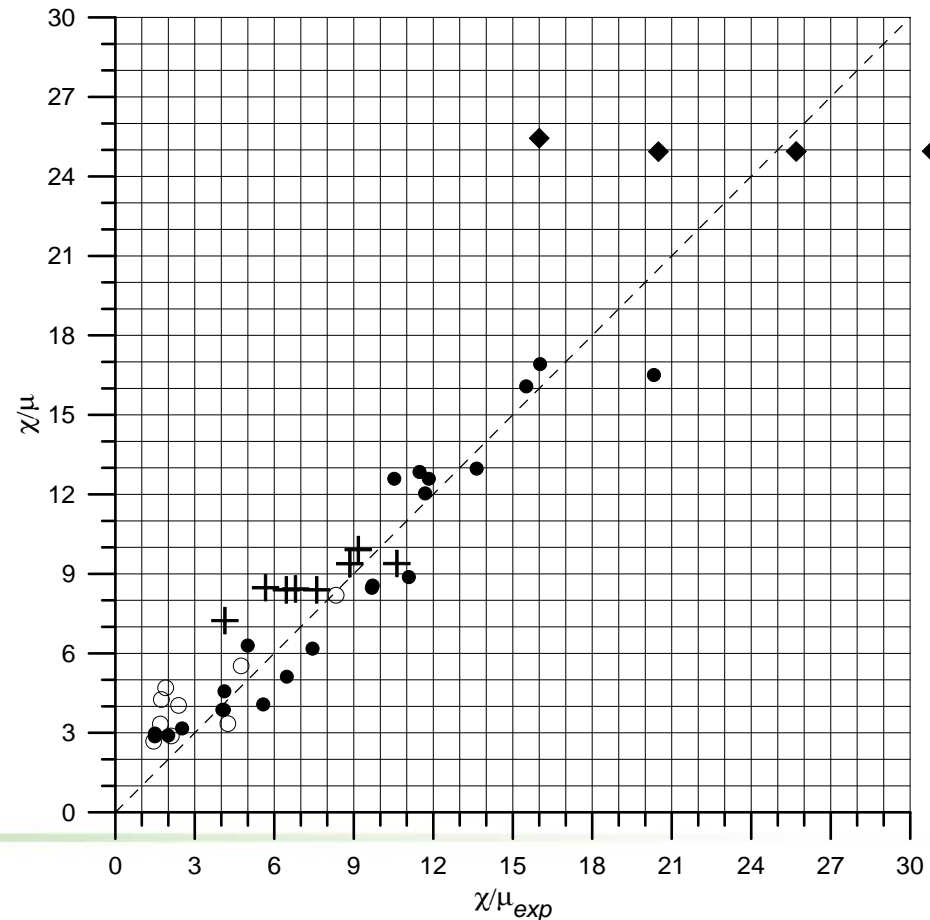
- χ = constant approach (Swift et al., 1986: "it seems best to employ a constant turbulence correction factor and gain the corresponding simplicity, rather than to carry more elaborate equations through a train of numerical computations whose accuracy is also limited to only a narrow range of experimental conditions").
- It has been demonstrated in a series of studies that reduced explosion pressure correlates with the *deflagration-outflow interaction (DOI) number*, that is the ratio of the turbulence factor, χ , to the discharge coefficient, μ , rather than with the turbulence factor alone (Tufano et al., 1981).
- The venting generated turbulence correlation (Molkov, 2000)

$$\chi / \mu = \alpha \cdot \left[\frac{(1 + 10 \cdot V_{\#}^{1/3}) \cdot (1 + 0.5 \cdot Br^{\beta})}{1 + \pi_v} \right]^{0.4} \cdot \pi_{i\#}^{0.6}$$

$$Br = \frac{F}{V^{2/3}} \cdot \frac{c_{ui}}{S_{ui}(E_i - 1)}$$

The DOI (χ/μ) numbers obtained by processing experimental data, χ/μ_{exp} , and determined by the correlation, χ/μ , for enclosures of different volume:

- Black circles – 0.02-1.00 m³ (initial pressures up to 7 bar);
- White circles – 2-11 m³;
- Crosses – 30-50 m³;
- Diamonds – 4000-8087 m³.



- The conservative form (139 tests – different mixtures)
- Valid in the full range of conditions.

NFPA 68 limits: $0.1 < P_{red} < 2$ bar,
 $P_{stat} < 0.5$ bar, $P_i < 1.2$ bar,
 $L:D < 2:1$, $K_G < 550$

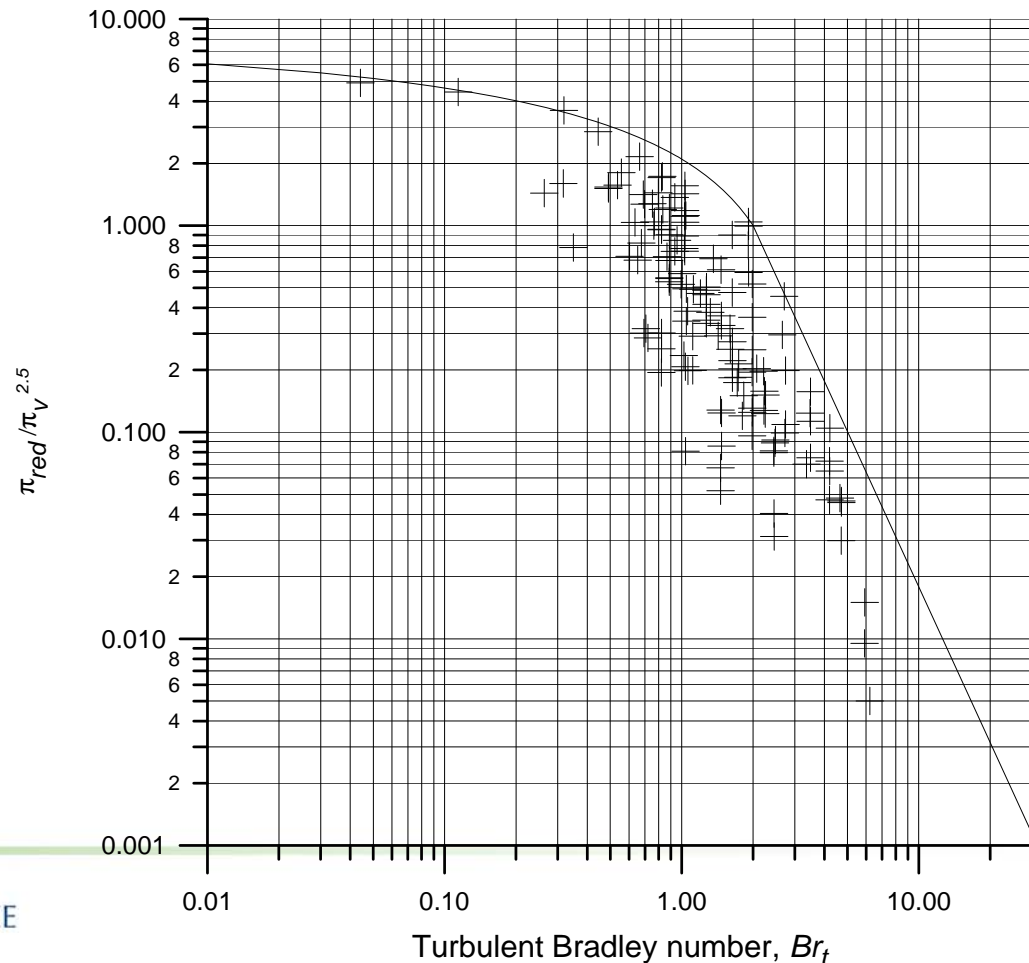
$$\frac{\pi_{red}}{\pi_v^{2.5}} = 5.65 \cdot Br_t^{-2.5} \quad \left(\frac{\pi_{red}}{\pi_v^{2.5}} \leq 1; Br_t \geq 2 \right)$$

$$\frac{\pi_{red}}{\pi_v^{2.5}} = 7.9 - 5.8 \cdot Br_t^{0.25} \quad \left(\frac{\pi_{red}}{\pi_v^{2.5}} > 1; Br_t < 2 \right)$$

$$Br_t = \frac{\sqrt{E_i / \gamma_u}}{\sqrt[3]{36\pi_0}} \cdot \frac{Br}{\chi / \mu}$$

$$\chi / \mu = \alpha \cdot \left[\frac{(1 + 10 \cdot V_{\#}^{1/3}) \cdot (1 + 0.5 \cdot Br^{\beta})}{1 + \pi_v} \right]^{0.4} \cdot \pi_{i\#}^{0.6}$$

$$Br = \frac{F}{V^{2/3}} \cdot \frac{c_{ui}}{S_{ui}(E_i - 1)}$$



Hydrogen only (updated χ/μ correlation)

Test	H ₂ , vol. %	Shape	V _i , m ³	F _i , m ²	Vent Area, F (m ²)					Reduced pressure, P _{red}				
					VST ^c	% ^d	NFPA ^e	% ^d	Exp ^f	VST ^c	% ^d	NFPA ^e	% ^d	Exp ^f
K-10-15-C	10	Sph	6.85	0.0177	0.0780	342	0.362	1948	0.0177	3.67	126	260.00	15900	1.625
K-10-15-R	10	Sph	6.85	0.0177	0.1070	506	0.448	2435	0.0177	3.67	224	260.00	22807	1.135
K-10-45-C	10	Sph	6.85	0.1590	0.2214	39	0.986	521	0.1590	0.54	79	6.49	2063	0.300
K-10-45-N	10	Sph	6.85	0.1590	0.4843	205	2.212	1292	0.1590	0.54	598	6.49	8340	0.077
K-15-15-C	15	Sph	6.85	0.0177	0.0753	326	0.223	1163	0.0177	5.34	46	260.00	6985	3.670
K-15-25-C	15	Sph	6.85	0.0191	0.1002	104	0.238	384	0.0491	4.20	27	46.90	1321	3.300
K-15-45-N	15	Sph	6.85	0.1590	0.4139	160	0.422	165	0.1590	2.68	113	6.49	417	1.255
K-20-15-C	20	Sph	6.85	0.0177	0.0536	203	0.185	947	0.0177	6.14	22	260.00	5069	5.030
K-20-25-C	20	Sph	6.85	0.0191	0.0819	67	0.196	300	0.0491	5.13	13	46.90	931	4.550
K-20-45-C	20	Sph	6.85	0.1590	0.1643	3	0.222	40	0.1590	3.74	1	6.49	75	3.700
P-1-C [94]	29.6	Cyl	0.95	0.20	0.2132	7	0.110	-45	0.2000	1.35	8	0.45	-64	1.250
P-2-C [94]	29.6	Cyl	0.95	0.30	0.4176	39	0.233	-22	0.3000	0.74	85	0.26	-35	0.400
SRI-30-F	30	Tun	37.4	7.48	11.95	60	1.112	-85	7.48	1.72	33	0.05	-96	1.300
SRI-20-F	20	Tun	37.4	7.48	11.82	58	2.434	-67	7.48	0.78	122	0.05	-85	0.280
SRI-15-F	15	Tun	37.4	7.48	7.48	0	3.127	-58	7.48	0.23	0	0.05	-77	0.220

Vent cover inertia

- Bartknecht (1993) suggests a mass of less than **10** kg/m².
- NFPA 68 standard suggested approximately **12** kg/m².
- Cooper (1998) stated that for volumes beyond 100 m³, doors with a mass of less than **20** kg/m² could be employed with little or no penalty on the predicted reduced pressure.
- In the UK, values of up to **25** kg/m² have been acceptable in the past, with some vents being more than **40** kg/m².
- The Russian standard SNiP II-90-81 allows the inertia of relief panel of **120** kg/m²!

V, m^3	F, m^2	F/A_{cs}	Br	χ / μ	χ	$w, \text{kg/m}^2$
0.1	0.04	0.20	31	4.5	2.7	< 0.31
10	1.76	0.38	59	8.6	5.2	< 16
100	11.62	0.54	84	12.3	7.4	< 113
1000	77.70	0.78	122	17.7	10.6	< 782

- The Le Chatelier-Broun principle can be formulated to cover general observations as: *any change in status quo prompts an opposing reaction in the responding system.*
- This principle works as well for vented deflagration phenomenon: *gas combustion dynamics in vented vessel responds to external changes in explosion conditions in such a way as to weaken the effect of external influence.*
- Below is an example based on use of the following theoretical formula:

$$\Delta\pi_m \propto (\chi \cdot S_u / \mu \cdot F)^2$$

- It follows from the formula that 10 increase of vent area F will lead to 100 decrease of overpressure $\Delta\pi_m$. However, experiments in 10 m³ volume vessel showed that **tenfold increase** in vent area is accompanied by **twofold increase** of turbulence factor χ . It results in “effective” vent area increase of only 10/2=5 times. Physical explanation of this observation is simple: the increase of vent area increases the disturbance of flame within the vessel by the venting process.

Hydrogen safety engineering and CFD

5

- 5a: Permeation
- 5b: Blowdown of high pressure hydrogen storage
- 5c: Spontaneous ignition of high pressure releases
- 5d: LES of premixed combustion (multi-phenomena model)

Permeation



- The permeation rate of hydrogen through a particular material depends on temperature, internal pressure and membrane thickness (mol/s/m²):

$$J = P_0 \exp(-E_0 / RT) \frac{\sqrt{P_r}}{l}$$

- Let us consider: does permeation from a composite tank with a non-metallic liner (type IV) in a garage present hazard?
- Three main phenomena will drive the dispersion of permeated hydrogen: buoyancy, diffusion, and ventilation. What can be done to simplify the problem solution?
- The perfect mixing equation can be used to calculate the allowable hydrogen release rate at steady state conditions (see next slide)

$$C_{\%} = \frac{100 \cdot Q_g}{Q_a + Q_g}$$

where $C_{\%}$ - volumetric concentration of hydrogen in air, % by vol.; Q_a - air flow rate, m³/min; Q_g - gas leakage rate, m³/min.

- If above formula is applicable then **the maximum allowable permeation rate** is

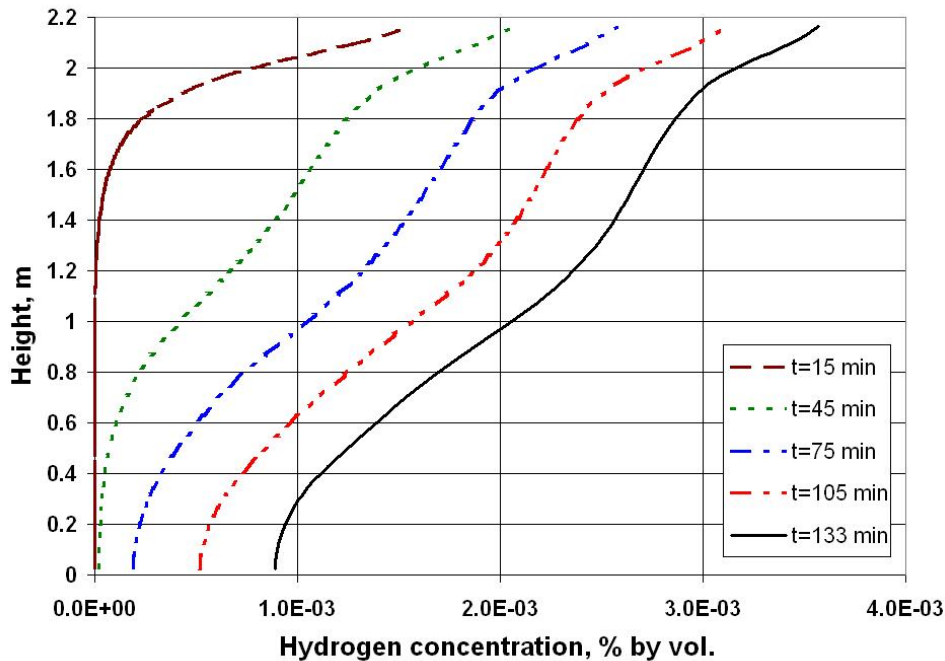
$$Q_{perm}^{max} = \frac{Q_a \cdot C_{\%}}{100 - C_{\%}} \cdot \frac{60 \cdot 10^6}{V \cdot f_a \cdot f_t}$$

where V - water capacity of hydrogen storage, L; f_a - aging factor, taken to be 2, for unknown aging effects; f_t - test temperature factor (equal 3.5 at test temperature 20°C, 4.7 - 15°C)

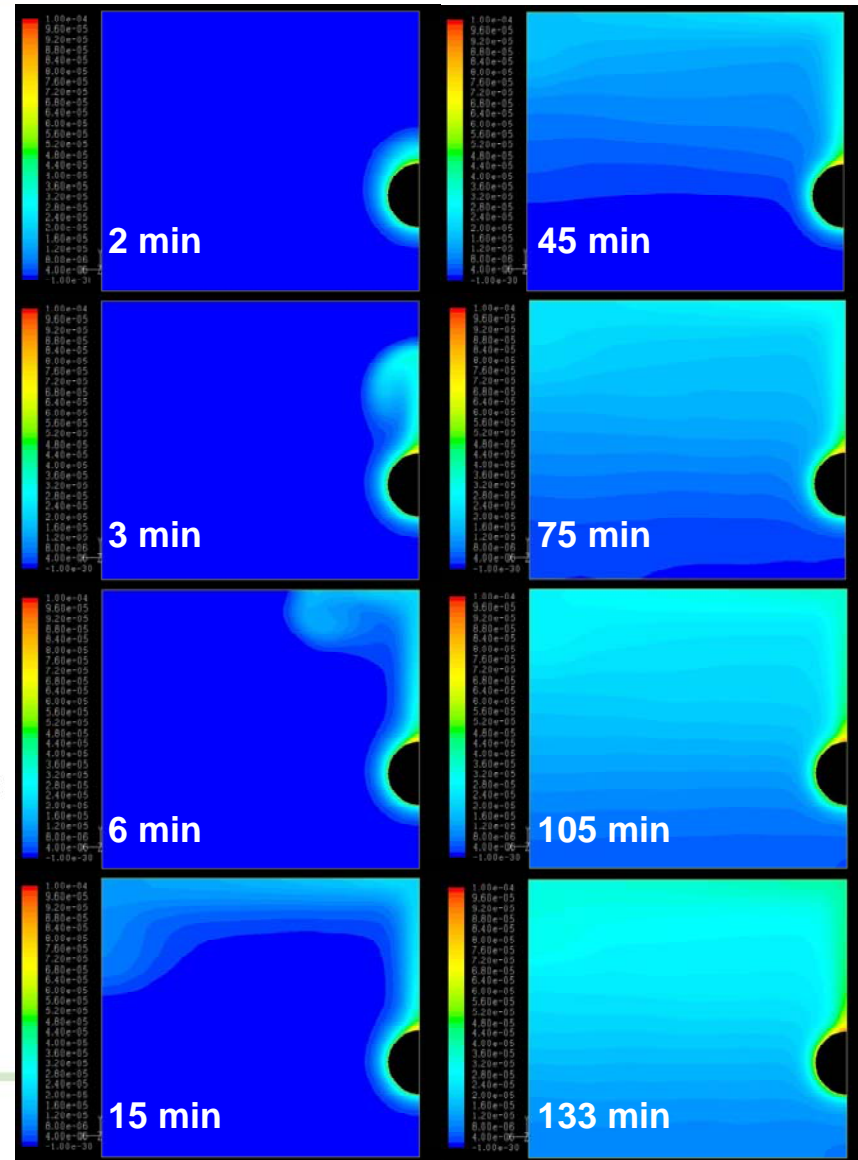
- Permeation is different phenomenon compared to plumes (buoyancy controlled) and jets (momentum controlled).
- Hydrogen releases in very small amounts equally along the surface of storage tank. Then it diffuses to locations with smaller concentration and buoyancy affects the flow pattern.
- Typical garage $L \times W \times H = 5 \times 3 \times 2.2$ m, $V = 33$ m³ with still air. Tank $L = 0.672$ m, $D = 0.505$ m, hemisphere at each end of $D = 0.505$ m ($V = 0.2$ m³). Floor clearance is 0.5 m. The surface area of the tank 1.87 m². $T = 298$ K. A permeation rate $J = 1.40 \times 10^{-6}$ mol/s/m² (1.14 NmL/hr/L of tank water capacity). This is close to the value presented in the draft of the UN ECE Regulation for type IV containers (1.0 NmL/hr/L).
- Time to reach lower flammability limit (LFL) of 4% in the closed garage with chosen storage tank and the permeation rate will be about **240 days** (in assumption that concentration of hydrogen is uniform, the statement yet to be proved).

- Characteristic time for hydrogen diffusion through the height of the garage is H^2/D_{H_2} (at 298 K as $D_{H_2}=7.79 \cdot 10^{-5} \text{ m}^2/\text{s}$). Indeed, $H^2/D_{H_2}=2.2^2/7.79 \cdot 10^{-5}=62051 \text{ s}$ or **0.7 days**.
- Thus, this estimate indicates that rather uniform distribution of hydrogen should be expected than a ceiling layer.
- The hydrogen release was modelled using a tiny volumetric source of hydrogen in a thin layer (two computational cell of 0.5 mm thickness) around the whole surface of tank. This is different from modelling of permeation by artificial plumes/jets with a mass fraction $Y_{H_2}=1$ at “release orifice” (our numerical experiments confirmed that there is no layer $Y_{H_2}=1$ on the tank’s surface). To match the specified permeation rate, the volumetric source term for hydrogen mass was $S_{H_2}=2.61 \times 10^{-8} \text{ kg m}^{-3} \text{ s}^{-1}$.
- CFD demonstrated: negligible stratification: (see next slide)

CFD: negligible stratification (no areas of 100% hydrogen)



The maximum at 133 min:
 tank top - 8.2×10^{-3} % by vol.;
 ceiling - 3.5×10^{-3} % by vol.



Key assumptions used in the HySafe estimation by Adams et al. (New tank: 15°C - 6 NmL/hr/L, 20°C - 8 NmL/hr/L):

- Permeated hydrogen disperses homogeneously.
- Reasonable minimum natural ventilation rate is 0.03ac/hr.
- Maximum permitted hydrogen concentration is 1% by vol.
- Maximum prolonged material temperature is 55°C.

Other suggestions:

- JARI for UN ECE HFCV GTR: at 15°C - 5 NmL/hr/L.
- SAE J2579:01 2009: end of life (55°C) - 150 NmL/min/vehicle (HySafe equivalent figure at 55°C, simulated end of life, SAE test conditions would be 90 NmL/min/vehicle)
- ISO/TS15869:2009 Option ii) Test E5: end of life (20°C) - 75 NmL/min/container

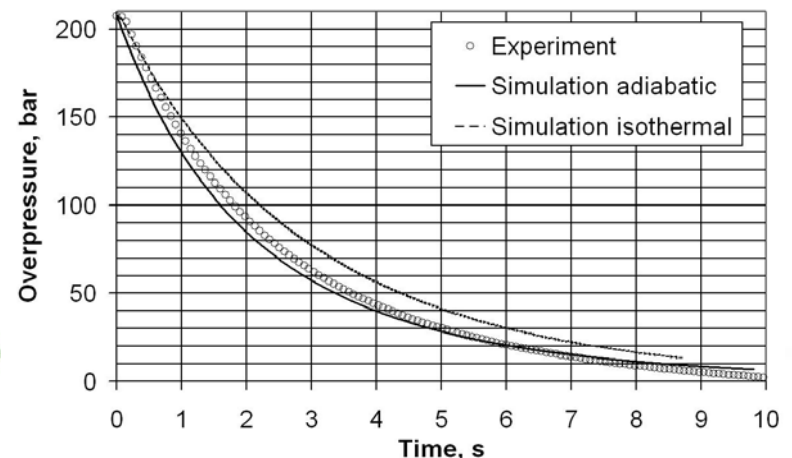
With this level of permeation rate the hydrogen dispersion in typical garage is not a problem!

Blowdown of high pressure hydrogen storage

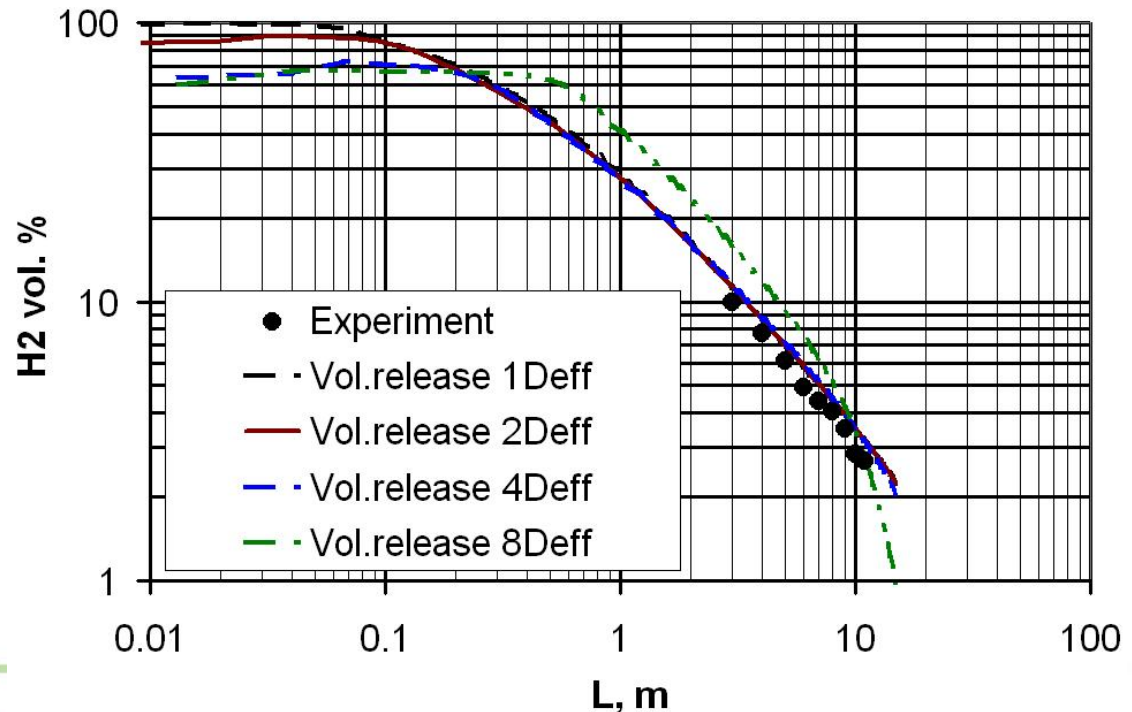


5b

- The problem of hydrogen dispersion is usually solved in two steps: 1) calculation of effective diameter, 2) use of CFD to simulate dispersion from the notional nozzle.
- If a characteristic time of gas flow from the nozzle of high storage to the size of the flammable envelope (4% by vol.) is less than a characteristic time of blowdown then the process of hydrogen dispersion is ***unsteady***.
- The HSL set up: two vessels of 98 litres each (3.025 kg of hydrogen), $P_i=208$ bar, $T_i=288$ K. Valve with throat wide open provided a minimum orifice diameter 9.5 mm in the pipeline.

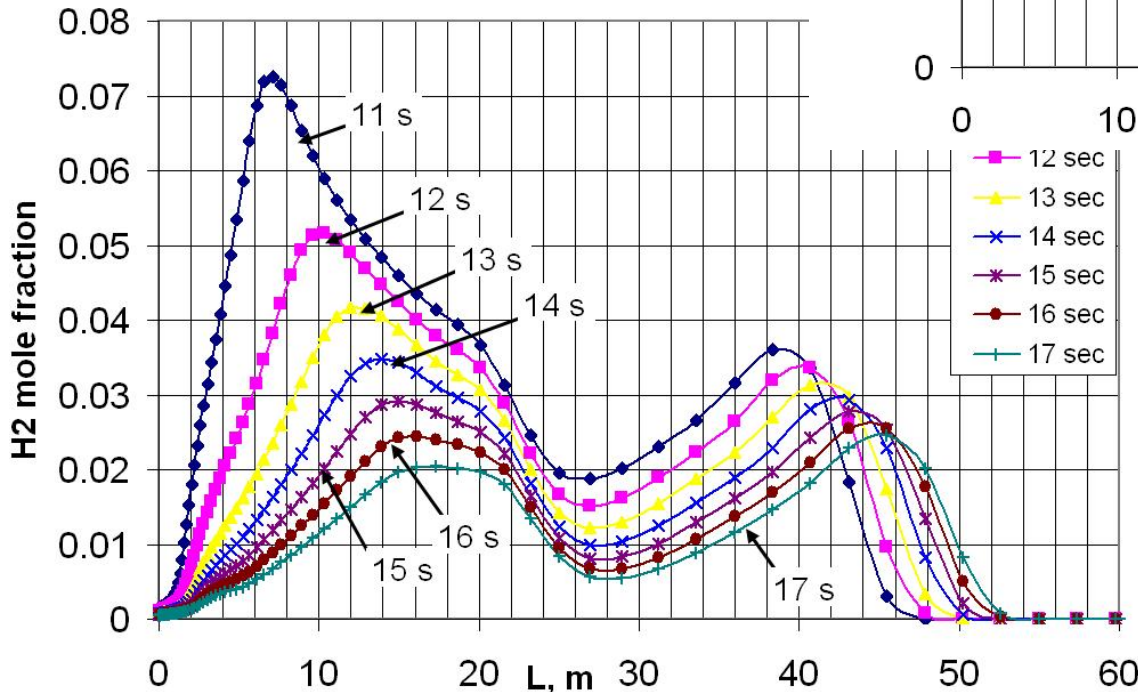
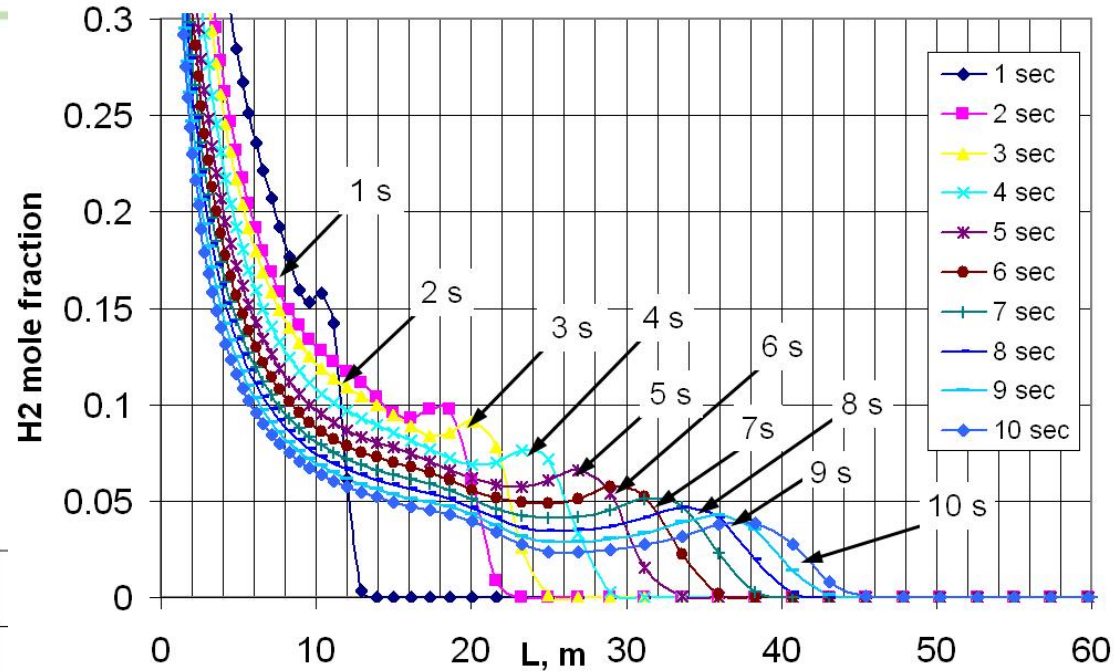


- To avoid simulation of changing with time diameter of the jet: changing volumetric sources of hydrogen mass, momentum, and energy in cylindrical volume with $L:D=1:1$ (pre-calculated using the adiabatic theory of underexpanded jet).
- Model calibration: HSL Run 7 (Shirvill et al., 2006), quasi-steady conditions,
 - $P_i=10.0$ MPa,
 - $T_i=14^\circ\text{C}$,
 - $m=45$ g/s,
 - nozzle $D=3$ mm.



Unsteady blowdown

**Steady jet correlation CR
(208 bar, 288 K, 9.5 mm,
10 s release): set-back
distance (4% vol.) is **50 m****



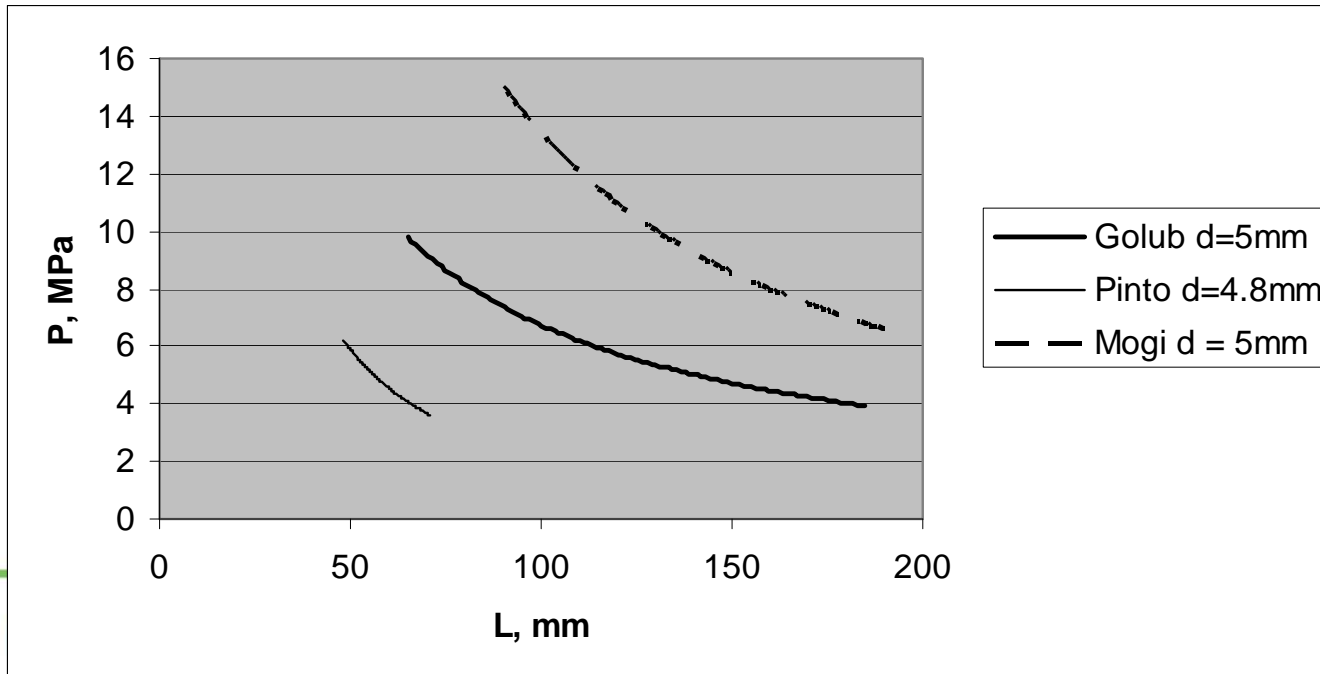
**CFD (unsteady
release): set-back
distance is **38 m only!****

**Clear advantage of
Hydrogen Safety
Engineering**

Spontaneous ignition of high pressure releases

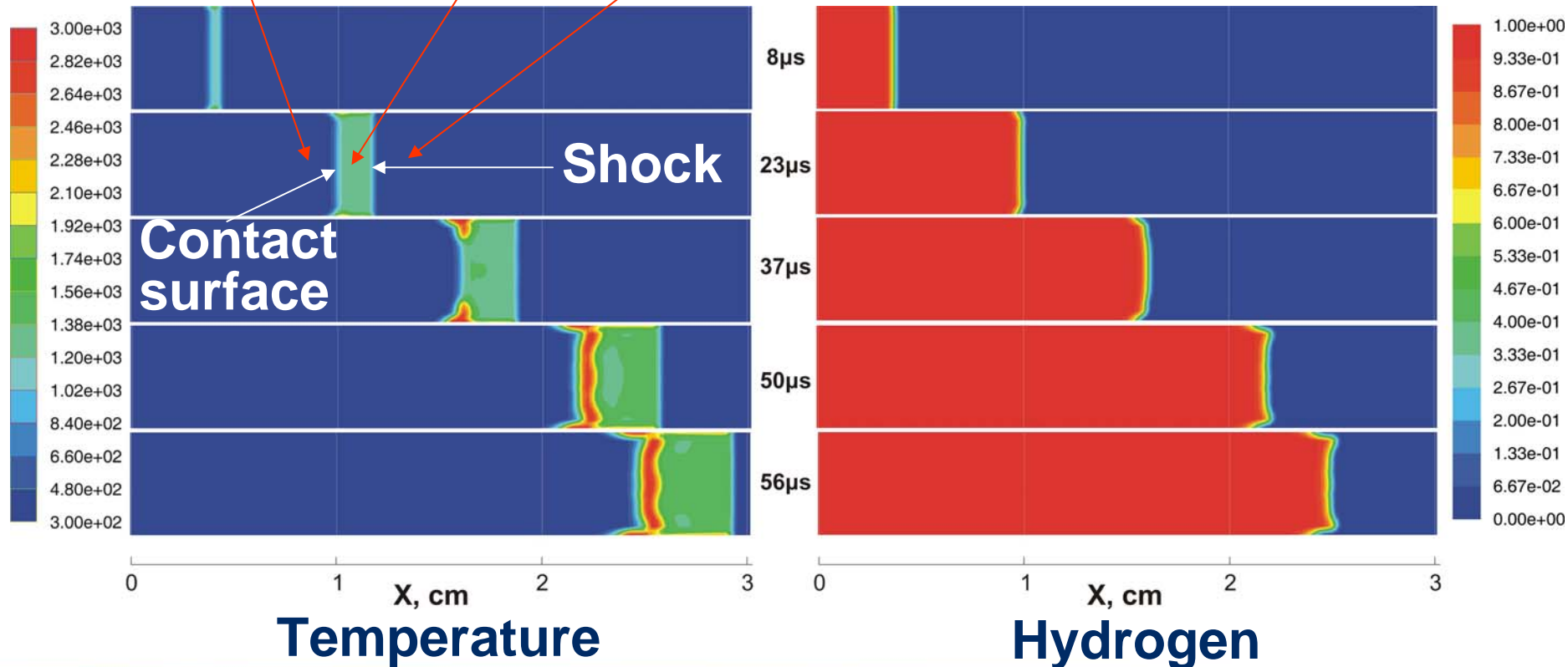


- Mogi et al. (2008): min **60 bar** (wetted by aqueous Na_2CO_3 solution (1%) internal pipe surface);
- Golub et al. (2007): min **40 bar** (dry surface);
- Pinto et al. (2007): min **40 bar** (50 mm, initial compression)
- Dryer et al. (2007): min **22.1 bar** (not flat rupture disk)
- Golub et al. (2009): **min 12 bar** (PRD geometry)

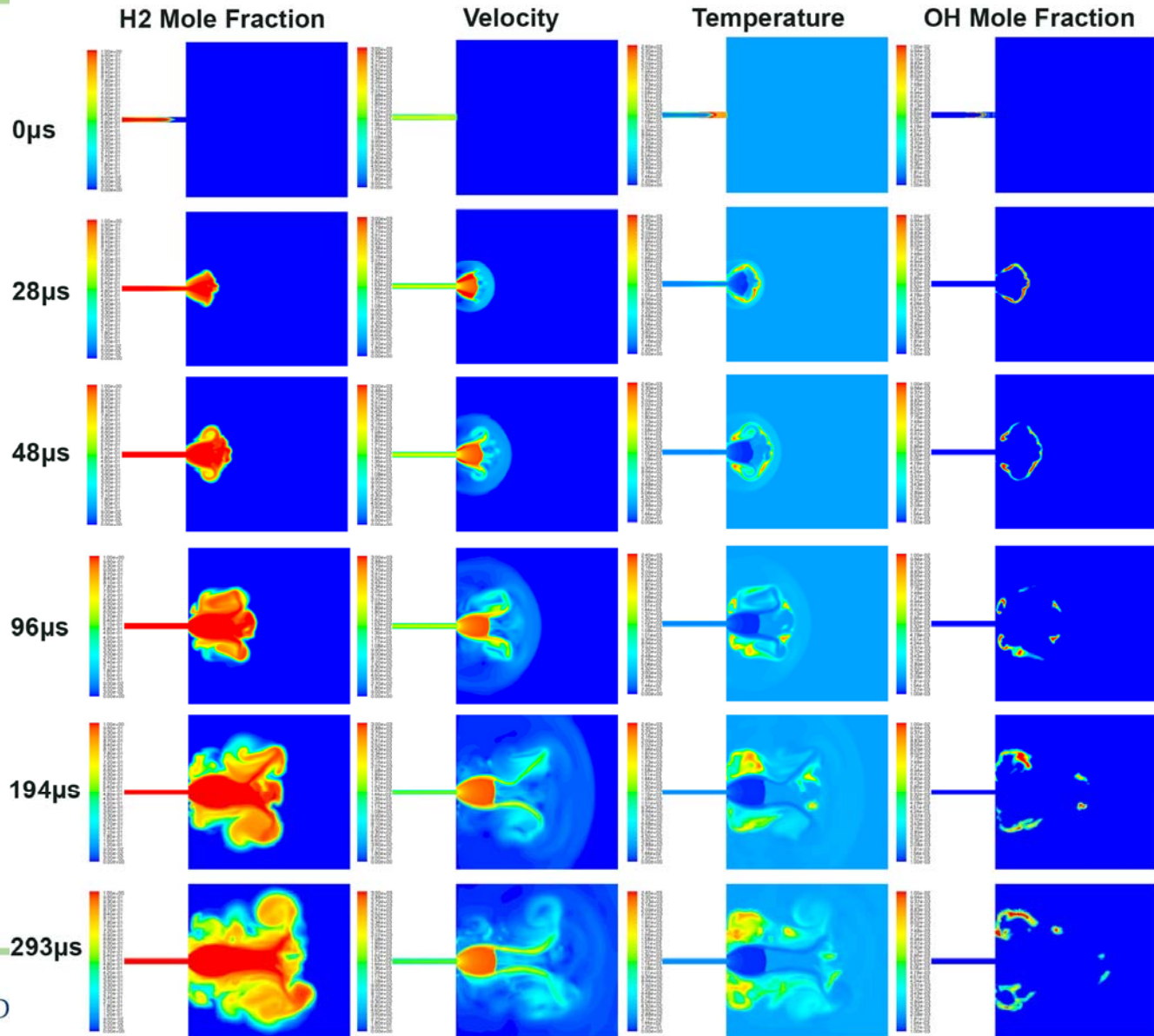


Wolanski and Wojcicki, 1972, “diffusion ignition mechanism”

Cold hydrogen Hot air Cold air



LES as a tool for Hydrogen Safety Engineering (PRD design)



Vortex induced “flame separation”

- Mogi et al. (2008, top) and LES snapshots of OH (bottom)
- Some difference due to: 1) wetting in the experiment of the inside surface of the tube by aqueous Na_2CO_3 solution (1%); 2) surface with channel instead of pipe in LES (entrainment)

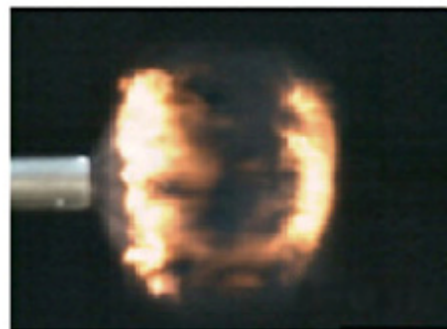
0 μs



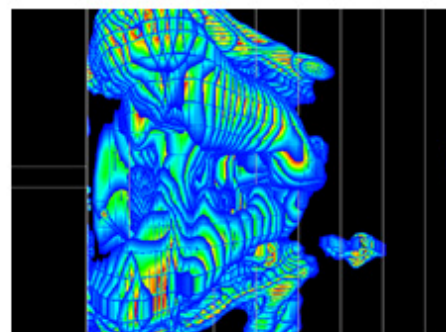
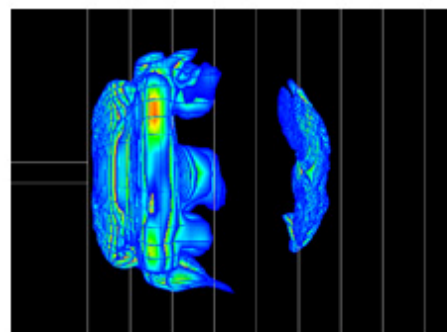
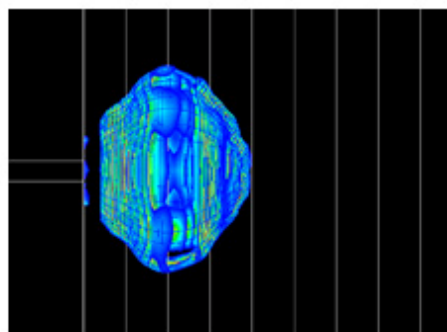
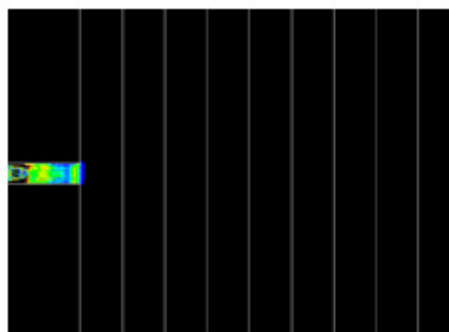
50 μs



100 μs



200 μs



LES of premixed combustion (multi-phenomena combustion model)



The key approaches for the closure of the combustion reaction rate in the flamelet regime are (Derek Bradley):

- **Flamelets with flame surface density,**
- **Heat release rates with presumed PDFs,**
- **Turbulent burning velocities, and**
- **Fractals.**

The following phenomena affecting *turbulent burning velocity model* are currently included into the model:

- **Flow turbulence (all scales),**
- **Turbulence generated by flame front itself (SGS),**
- **Preferential diffusion effects (leading point concept) for lean hydrogen-air mixtures (SGS), and**
- **Fractals structure of turbulent flame surface (SGS)**

- The historically **first** group of turbulent burning velocity models assumes dependence of the turbulent burning velocity on the ratio of root mean square (rms) velocity to laminar burning velocity, u'/Su , only. Unfortunately, such simplified models, when implemented in the premixed LES code, are not able to reproduce even acceleration of unconfined flames.
- The **second** group of models introduces an additional dependence of turbulent burning velocity on turbulence scale(s), which are difficult to interpret and which are calibrated by small-scale experiments thus limiting their extrapolation to large-scale problems.
- The last group of fractals models introduces dependence of the turbulent burning velocity on the transient outer cut-off (integral scale) and the inner cut-off, e.g. laminar flame thickness or Kolmogorov scale or Gibson scale etc.
Meaningful comparisons between the first and the last groups are not possible (North and Santavicca, 1990).

- The renormalization group (RNG) theory (Yakhot and Orszag, 1986) is applied to calculate both turbulent burning velocity and viscosity. The RNG method is favoured for its ability to model flows in both limits - laminar and turbulent.
- The **original** Yakhot's equation for turbulent flame propagation velocity is a basis of the model (no empirical coefficients)

$$S_t = S_u \cdot \exp\left(\frac{u'}{S_t}\right)^2$$

- The criticism of the Yakhot's formula could be bounced back to sceptics on inappropriate use of the equation. The modified equations used in the LES model (SGS – sub-grid scale)

$$S_t = S_t^{SGS} \cdot \exp\left(\frac{u'}{S_t}\right)^2$$

Turbulence generated by flame front itself (1/2)

- The recognition that the turbulent flame itself generates additional turbulence first came in 1951 (Karlovitz *et al.*).
- The unburned mixture passes through the flame front with a laminar burning velocity S_u . However, the combustion products leave the flame front with velocity $E_i S_u$, where E_i is combustion products expansion coefficient (7-8 for fast burning hydrogen-air mixtures). Thus, the flame front constitutes a flow source that introduces a velocity into the gas flow of the magnitude $(E_i - 1) \cdot S_u$. In turbulent flame brush the flamelets are subject to fluctuating motions, and hence the orientation of this flame-induced velocity fluctuates also.
- An upper limit of flame-generated turbulence is assessed as

$$u' = \frac{(E_i - 1) \cdot S_u}{\sqrt{3}}$$

Turbulence generated by flame front itself (2/2)

Consequently, the upper limit for a flame wrinkling factor due to the turbulence generated by flame itself is estimated as

$$\Xi_K^{\max} = \frac{S_t}{S_u} = \frac{u'}{S_u} = \frac{(E_i - 1)}{\sqrt{3}}$$

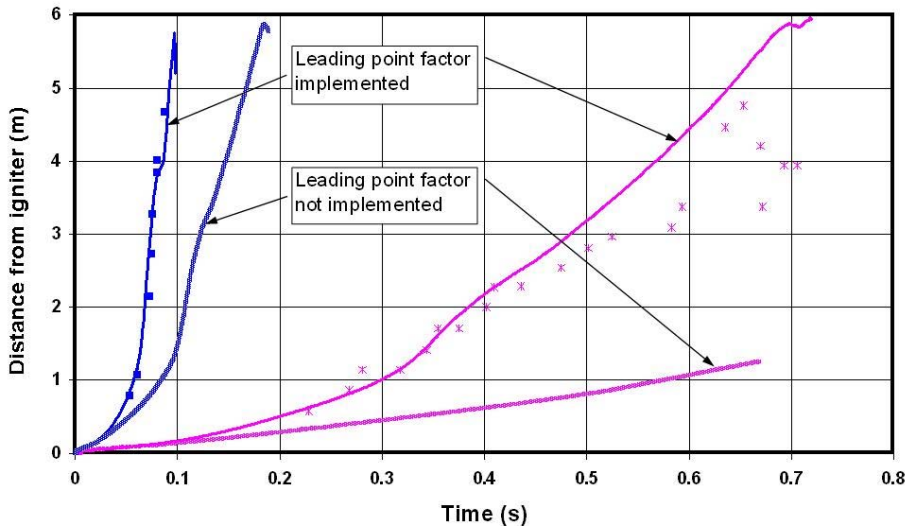
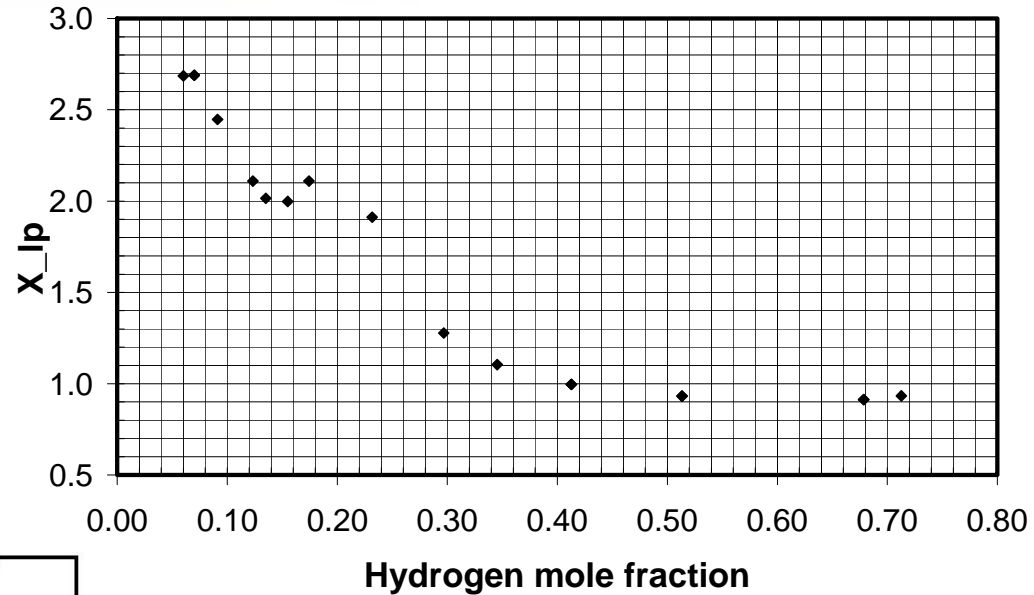
Gostintsev *et al.* (1988): a critical radius for transition from laminar to fully developed turbulent flame for near stoichiometric hydrogen-air mixtures is about $R^*=1$ m. The following formula is applied for transient value of flame wrinkling factor due to the self-induced by flame turbulence

$$\Xi_K = 1 + \left(\psi \cdot \Xi_K^{\max} - 1 \right) \cdot \left[1 - \exp\left(-\frac{R}{R^*} \right) \right]$$

where R is distance from the ignition source, and $\psi < 1$ is the only calibration coefficient of the model (how close the maximum theoretical value could be achieved).

- Turbulent flame is an aggregate of strained flamelets of different curvature. For particular mixture composition there is a curvature radius with maximum burning rate. Thus, flamelets of such curvature will lead propagation of the turbulent flame. The correction factor to laminar burning velocity associated with this mechanism (subscript “ l_p ” stands for “leading point”), is adopted from Zimont and Lipatnikov (1995), who used the formulation by Kuznetsov and Sabelnikov (1990).
- In the multi-phenomena turbulent burning velocity model it is assumed that for initially quiescent mixture the preferential-diffusive instability develops linearly with radius and reaches maximum at half of critical radius R^* and remains constant after that.

Preferential diffusion
correction to SGS
turbulent burning velocity



Example of the correction
effect (Whitehouse et al., 1996)

- The fractal theory was developed for description of highly contorted and roughened curves and surfaces.
- The nature of combustion in the regime for the Peclet number (flame radius/flame thickness) above the critical is referred as fractal-like flame wrinkling and is responsible for a further increase of the turbulent burning velocity (Bradley, 1999).
- According to fractals the flame surface area of outward propagating turbulent flame will grow not as R^2 valid for laminar flame, but faster as $R^2 \cdot R^{D-2}$, where D is the fractal dimension (experimental data 2.11-2.35). The empirical parameterization of the fractal dimension as a function of (u'/S_u) (North and Santavicca, 1990) is applied in the model

$$D = \frac{2.05}{u' / S_u + 1} + \frac{2.35}{S_u / u' + 1}$$

- The integral scale of the problem R , e.g. flame radius, is the **outer cut-off**. The **inner cut-off** is chosen currently as a laminar flame front thickness. The effect of changing temperature of unburned mixture and explosion pressure on the inner cut-off was calculated assuming ν , where ν is kinematic viscosity. To exclude a stage of quasi-laminar/transitional flame propagation after ignition up to the critical radius R^* , when fractals theory can be hardly applied, it can be shown that a wrinkling factor due to the fractals nature of the turbulent premixed flame surface to be applied after R^* is

$$\Xi_f = \left(\frac{R \cdot \varepsilon_{R^*}}{R^* \cdot \varepsilon} \right)^{D-2}$$

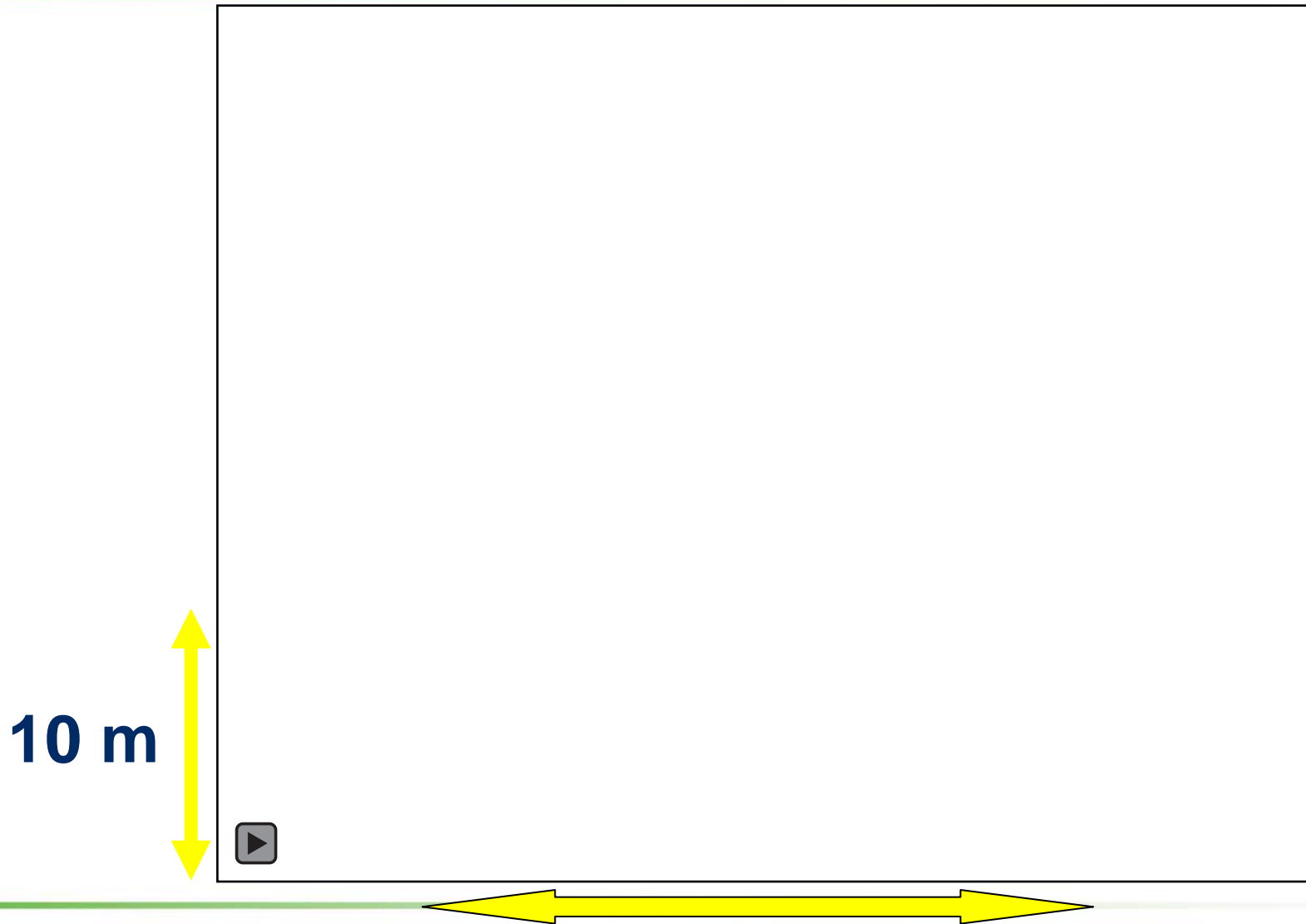
Final equation

- The multi-phenomena turbulent burning velocity model for LES of premixed combustion has been developed during the last decade at the University of Ulster. The equation casts as

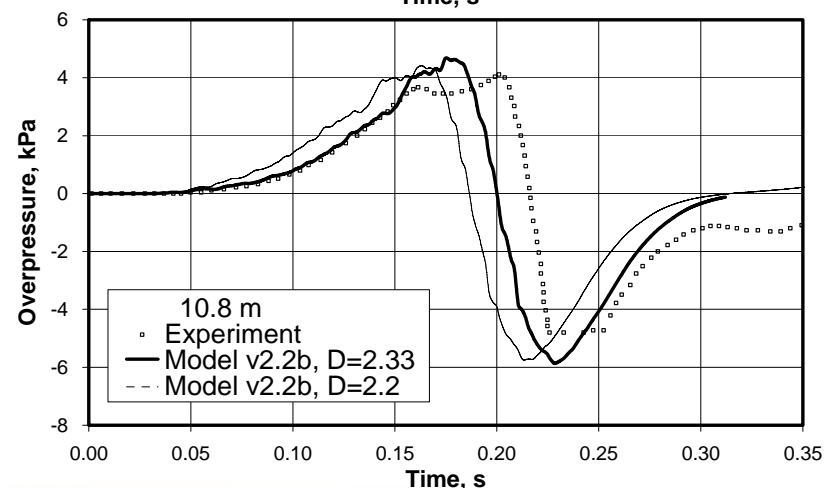
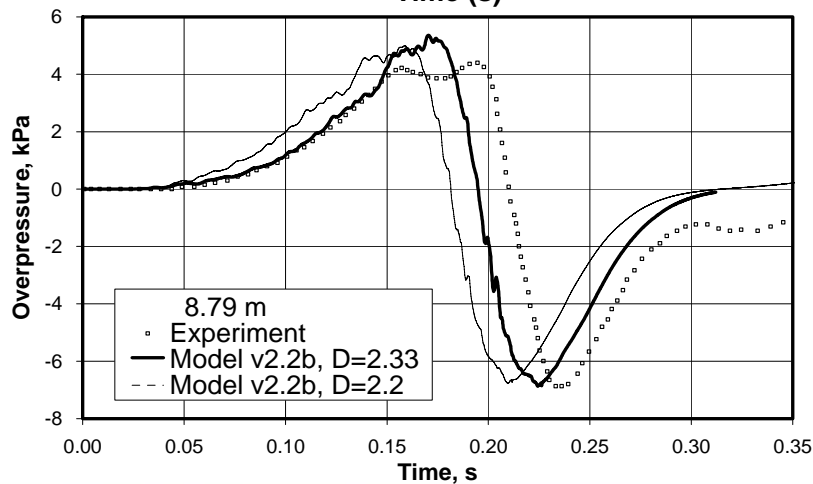
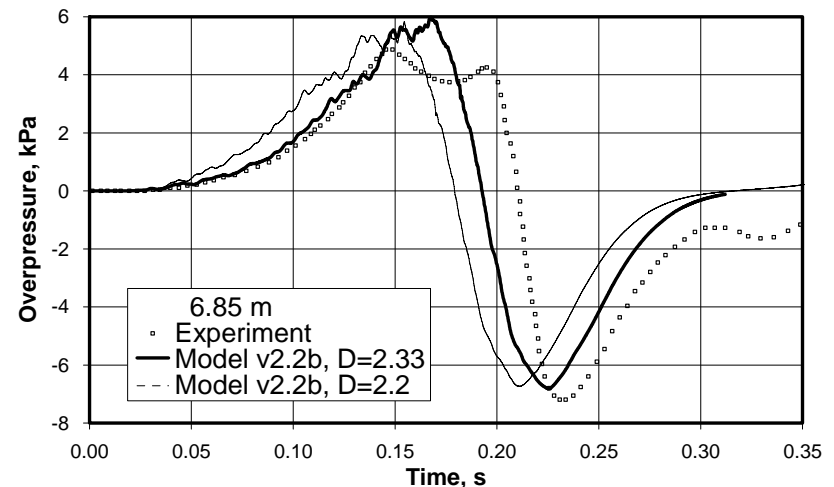
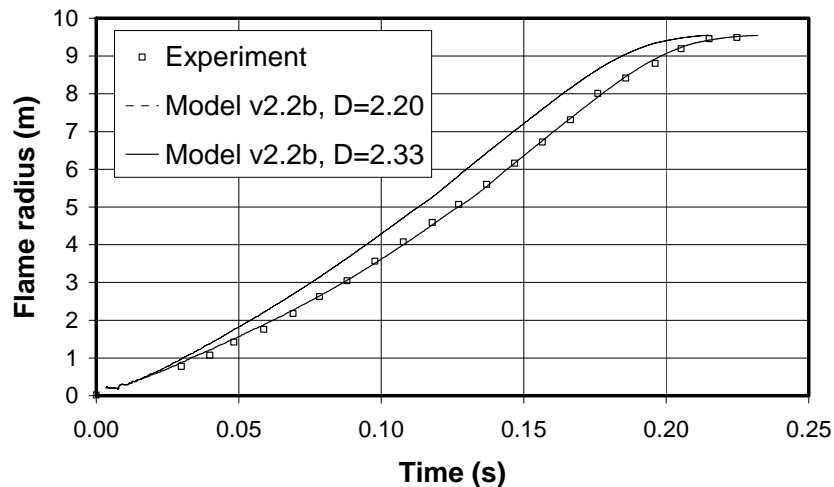
$$S_t = [S_u \cdot \Xi_K \cdot \Xi_{lp} \cdot \Xi_f] \cdot \exp\left(\frac{u'}{S_t}\right)^2$$

- In addition to the flow turbulence in unburned mixture and the dependence of laminar burning velocity of pressure, temperature, and mixture composition, the model for the first time accounts, in an aggregate manner, for three other interrelated **SGS** mechanisms of increase of flame front area:
 - turbulence generated by flame front itself,
 - preferential diffusion effect in turbulent brush, and
 - fractal growth of turbulent flame front area

Open atmosphere (1/2)

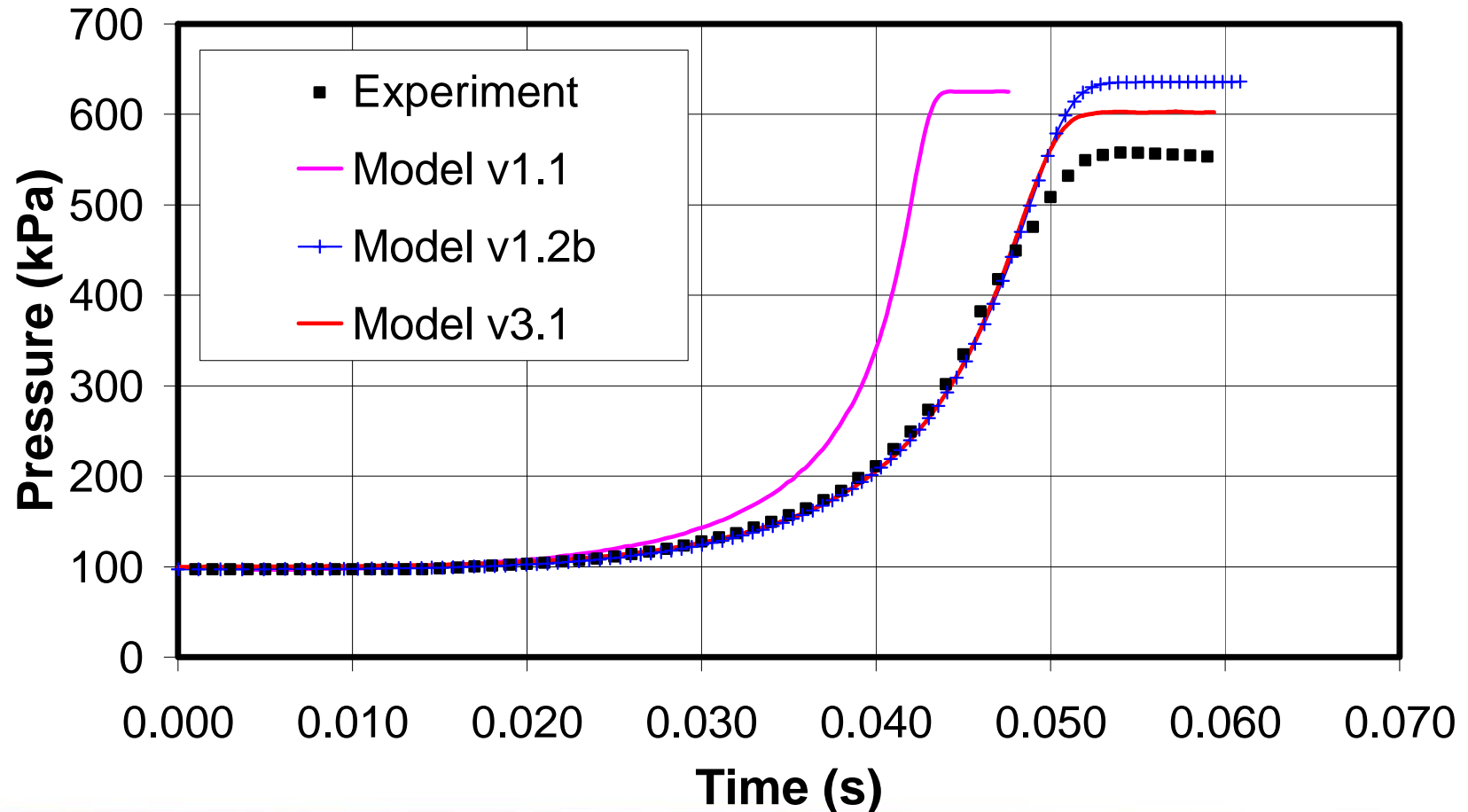


Hemisphere 10 m diameter (Fraunhofer ICT)



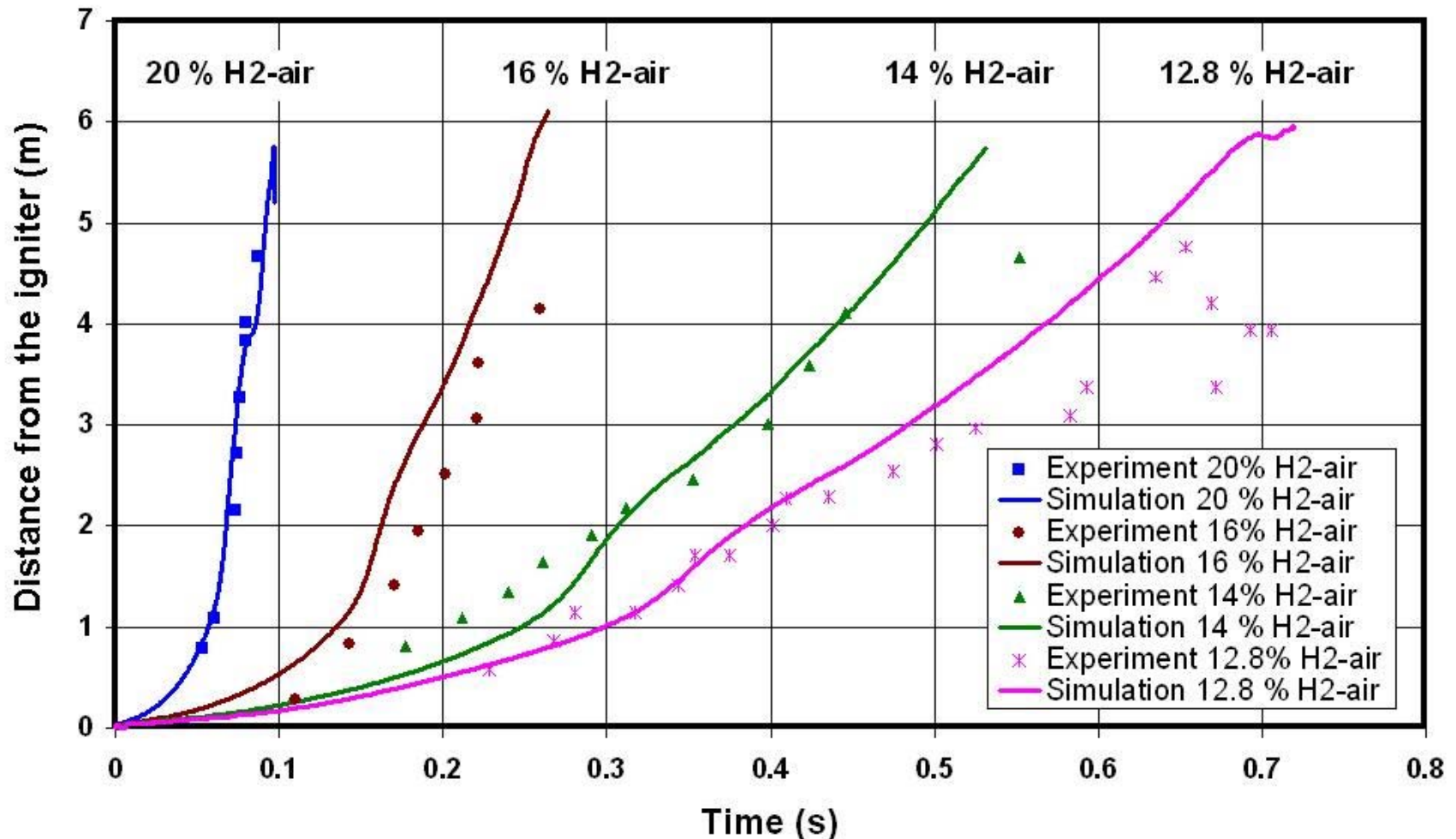
Closed vessel 1/3

Kumar et al. (1983): $V=6.37 \text{ m}^3$, $D=2.3 \text{ m}$, $T=373 \text{ K}$, $p=97 \text{ kPa}$

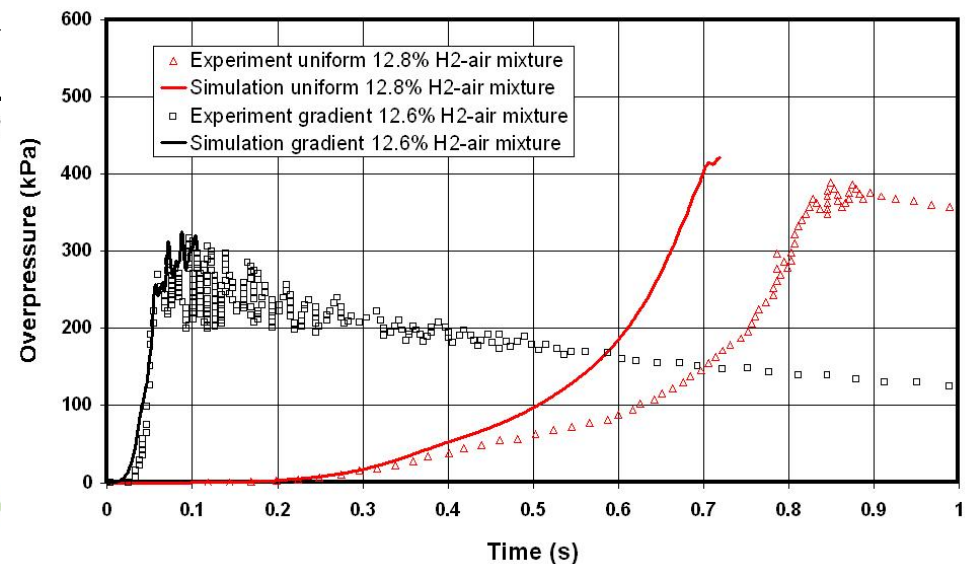
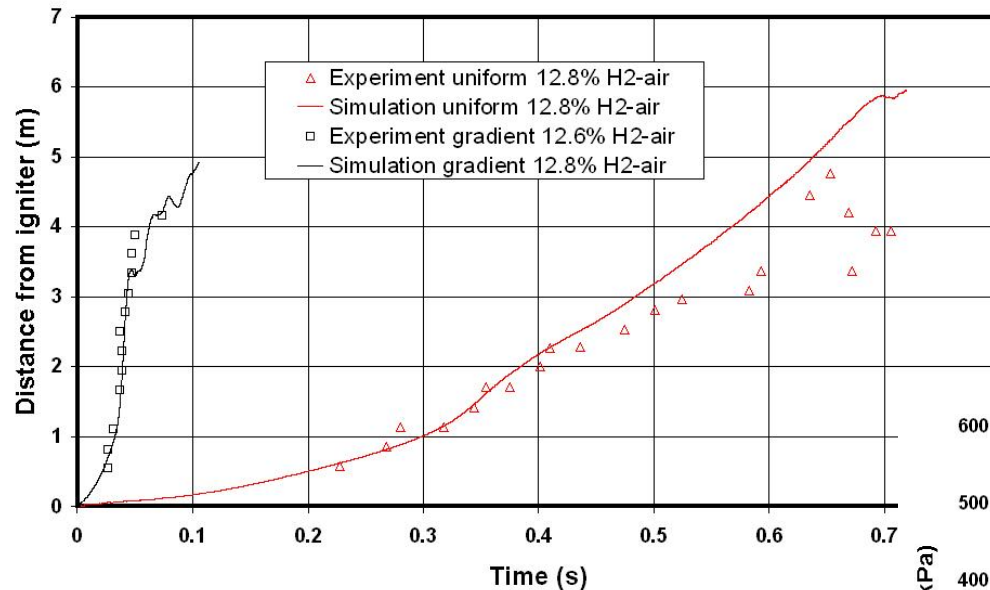


Closed vessel 2/3

Whitehouse et al. (1996): $L=5.7$ m; $D=1.5$ m ($V=10.1$ m³),
uniform 12–20% mixture

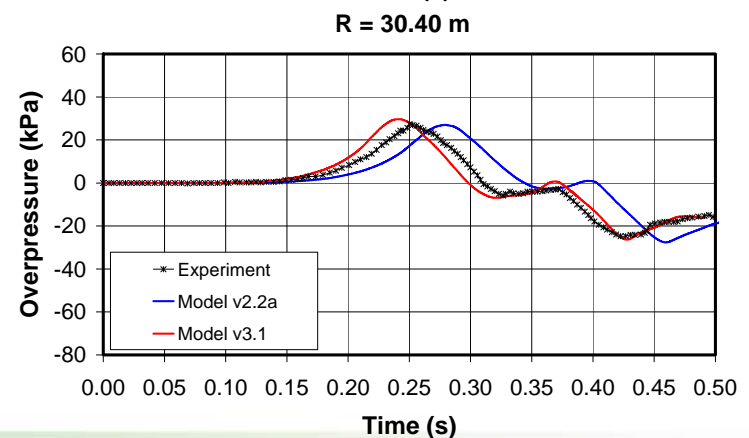
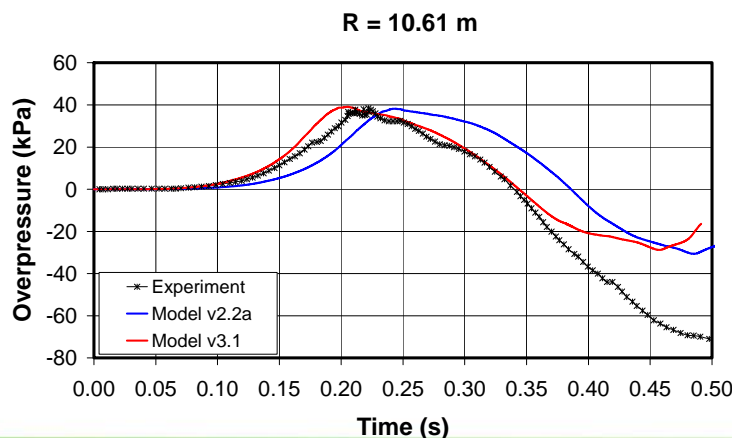
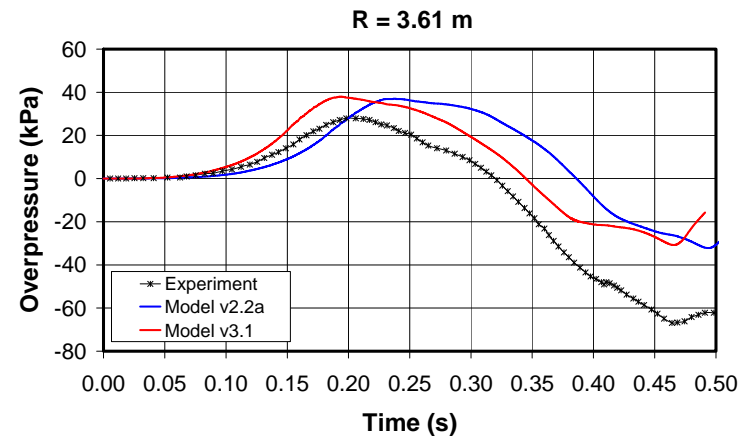
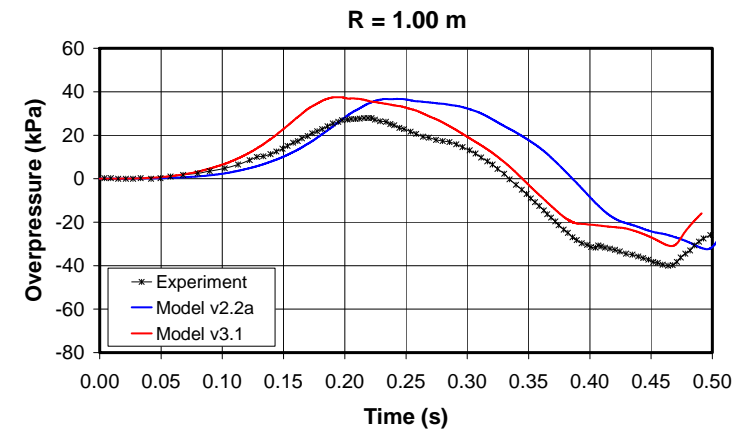


Whitehouse et al. (1996): $L=5.7$ m; $D=1.5$ m ($V=10.1$ m³),
uniform (12.8%) vs non-uniform (average 12.6%) mixture

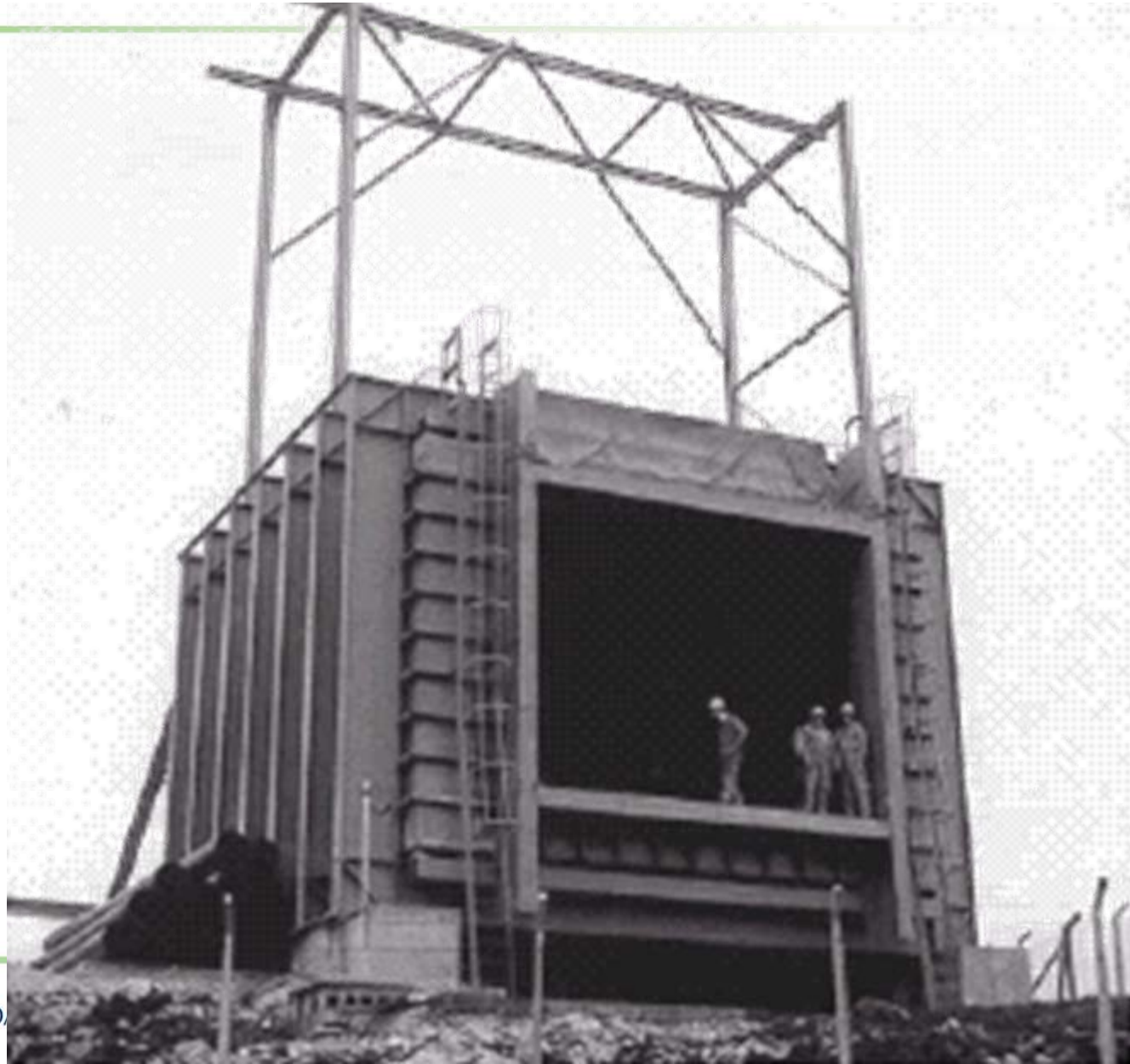


Tunnel 78.5 m length

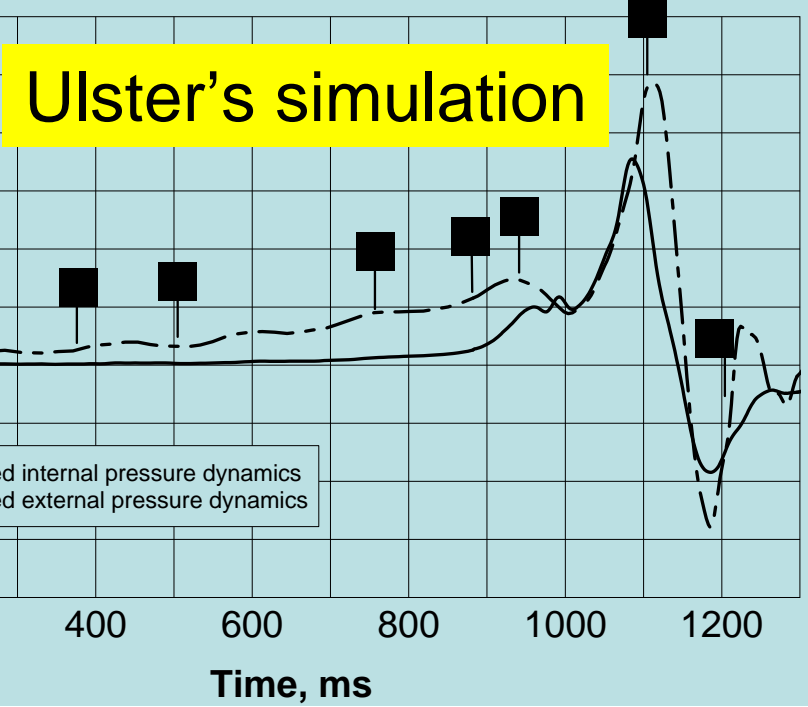
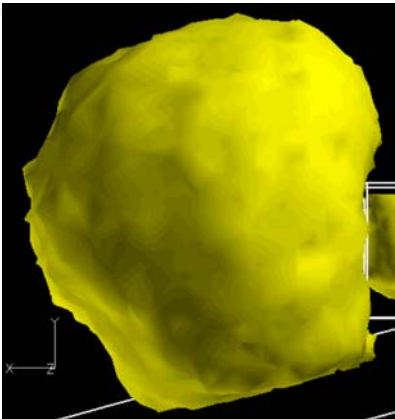
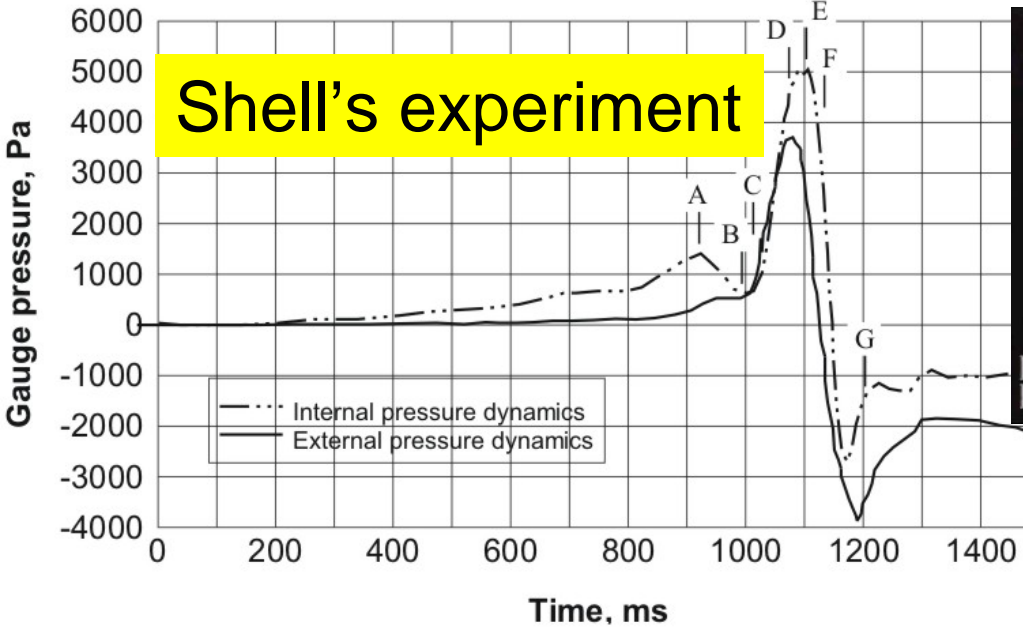
Groethe et al. (2005): $L=78.5$ m, $H=1.84$ m, horseshoe shape cross sectional area of 3.74 m². Example: uniform **20%** hydrogen-air mixtures of 37.4 m³ volume (10 m long cloud)



Shell SOLVEX:
 $V=547 \text{ m}^3$;
10.5% methane-air
mixture;
Initially open vent;
Back-wall ignition.



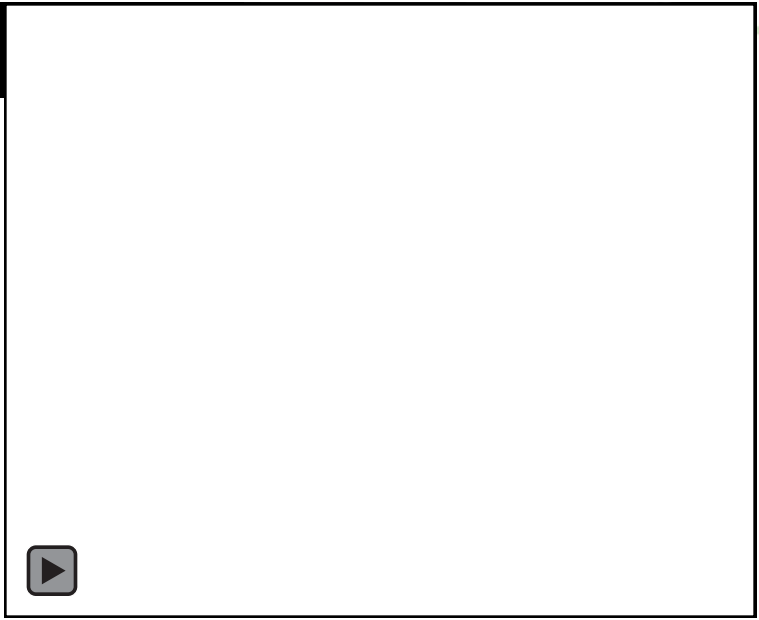
Coherent deflagrations (2/3)



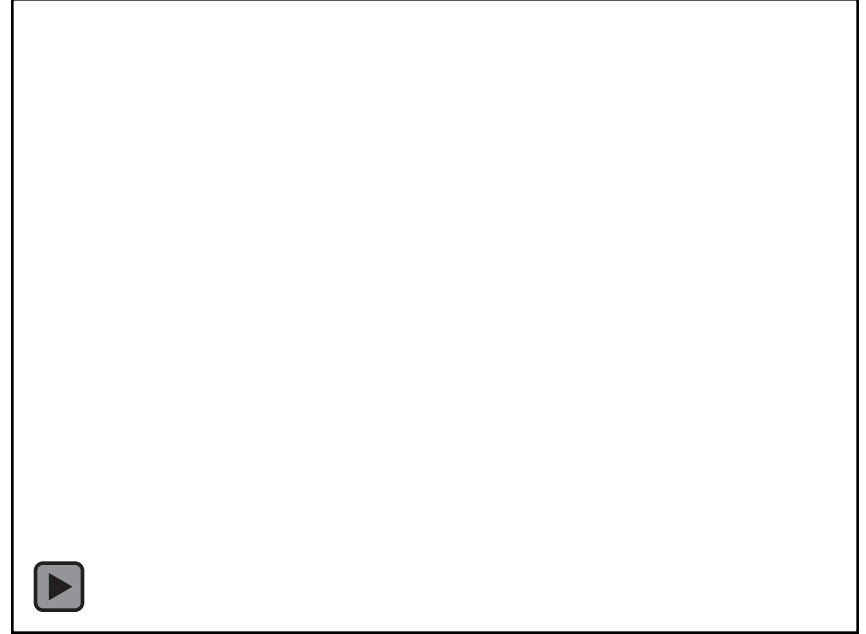
External explosion
(in 100 ms):

$$ext = 1 \quad 2$$

Shell 3



Ulster LES model



Shell 4

